Applied Mathematical Modelling 125 (2024) 241–260

Contents lists available at ScienceDirect

Applied Mathematical Modelling

journal homepage: www.elsevier.com/locate/apm

Mathematical analysis of a multiscale hepatitis C virus infection model with two viral strains

Xia Wang [a], Qing Ge [a], Hongyan Zhao [a], Libin Rong [b,*]

[a] College of Mathematics and Statistics, Xinyang Normal University, Xinyang, 464000, China
[b] Department of Mathematics, University of Florida, Gainesville, FL 32611, USA

ARTICLE INFO

Keywords:
Hepatitis C virus
Multiscale model
Infection age
Drug-resistant
Intracellular viral RNA

ABSTRACT

Direct-acting antiviral agents (DAAs) have shown higher cure rates for treating hepatitis C virus (HCV) by directly interfering with different steps of the HCV life cycle. To optimize drug combinations and accurately quantify the antiviral effect of DAAs treatments, mathematical models should include the intracellular virus replication processes. In this study, we develop a two-strain multiscale age-structured model that includes intracellular viral RNA replication and extracellular viral infection. We prove the existence, positivity, and boundedness of the solution, and derive the conditions for the existence and stability of the three steady states (non-infection steady state, boundary steady state, and coexistence steady state). Under certain biologically reasonable assumptions, we obtain the approximate solutions of the viral load decline of the two virus strains (sensitive and drug-resistant virus strains) during treatment, and the long-term approximation is shown to be in good agreement with the solution of the original model. We also carry out numerical simulations using the long-term approximate solution, providing insights into the influence of antiviral effects on the viral load change of the two virus strains during treatment with DAAs.

1. Introduction

Hepatitis C virus (HCV) infection is a global epidemic infectious disease that poses a significant threat to human health. HCV is a flavivirus single-stranded positive strand RNA virus and primarily transmitted through blood. According to global health organization statistics, the prevalence of HCV infection is around 2.8%, with approximately 185 million individuals infected and 35,000 new cases occurring annually [1]. Globally, an estimated 58 million people have chronic HCV infection, with about 1.5 million new infections occurring per year [2]. Chronic HCV infection is a leading cause of liver cirrhosis, hepatocellular carcinoma, end-stage liver failure, liver transplantation, and final liver failure. Achieving long-term sustained virological response (SVR) is critical in preventing disease progression, which refers to the absence of HCV RNA in the serum 24 weeks after treatment.

Currently, there is no vaccine available to prevent HCV infection. The standard treatment used to be a combination of pegylated interferon (PEG-IFN) and ribavirin (RBV). However, only about 50% of patients with HCV genotype 1 infection (the predominant genotype in North America and Europe) achieve SVR [3]. New treatment options focus on the use of direct-acting antiviral drugs

* Corresponding author.
E-mail address: libinrong@ufl.edu (L. Rong).

https://doi.org/10.1016/j.apm.2023.08.035
Received 28 May 2023; Received in revised form 9 August 2023; Accepted 24 August 2023

Available online 30 August 2023

(DAAs), which target various stages of the HCV life cycle [4]. DAAs have several advantages, including high SVR rates, low recurrence rates, and few adverse reactions, making them a promising treatment option for HCV-related cirrhosis patients. However, HCV infection is prone to developing drug-resistant mutations within days or weeks of DAA monotherapy, leading to ineffective treatment. To combat this, multiple drugs with different modes of action are used to enhance antiviral activity and reduce the likelihood of drug resistance. Using multiple drugs is currently the standard strategy for antiviral treatment [5].

Mathematical models have been developed to study the dynamics of HCV infection under treatment [6–9]. Multiple drug treatments have been shown to significantly improve the clinical efficacy of HCV, and mathematical models can accurately quantify the antiviral effect of such treatments, facilitating optimization efforts [10–12]. To more accurately describe and quantify the different antiviral effects of anti-HCV drugs, some researchers have proposed multiscale models, which study the replication process of intracellular viruses and corresponding antiviral effects in different stages [10–12]. Age-structured models have been used to study the infection kinetics of various viruses in the host [10,13,14]. Such models are typically expressed using partial differential equations (PDEs). Accurately quantifying the antiviral effect from clinical data of multi-drug therapy is necessary, and multiscale models can study the dynamics of virus infection between cells, including the process of virus replication in cells, according to the drug's potential mechanisms of action [15,16]. For example, Guedj et al. considered intracellular HCV replication/degradation and established an age-structured multiscale model of HCV infection [17]. Reinharz et al. proposed the HCV multiscale model based on this feature and estimated parameter values from clinical data under multi-drug treatment [15]. Zitzmann et al. developed an intracellular replication model involving HCV RNA secretion/release and viral assembly, and their study suggested that low levels of HCV RNA secretion may persist as long as intracellular RNA is available, possibly explaining the availability of plasma HCV RNA at the end of treatment, even in patients who eventually achieved sustained virologic response [18]. Many existing models in the literature regard infected cells as "black boxes" that produce new virus particles after infection, without considering other factors such as replication/degradation of virus RNA in infected cells. However, these intracellular processes may play a key role in studying HCV dynamics under DAAs treatment since they are direct targets of DAAs [10].

In this paper, we develop a two-strain multiscale model that includes intracellular viral RNA replication and extracellular viral infection to study the dynamics of HCV infection under DAAs treatment. We prove the existence, positivity, and boundedness of the solution of the model and calculate three steady states (the infection-free steady state, boundary steady state, and coexistence steady state) of the model, respectively. Under certain assumptions, we obtain analytical approximations of the viral load decline of the two virus strains (drug-sensitive virus and drug-resistant virus) after the start of treatment. We find that one of the approximations agrees well with the solution of the original model. Using the analytical long-term approximate solution, we carry out numerical simulations to investigate the influence of different antiviral effects of DAAs on the changes of the two strains of viruses during treatment.

2. Model formulation

The basic model for studying HCV infection dynamics under therapy is described by the following ordinary differential equations (ODEs) [19,20]:

$$\begin{cases} \dfrac{dT(t)}{dt} = s - \beta V(t)T(t) - dT(t), \\ \dfrac{dI(t)}{dt} = \beta V(t)T(t) - \delta I(t), \\ \dfrac{dV(t)}{dt} = (1-\varepsilon)pI(t) - cV(t), \end{cases} \tag{2.1}$$

where the variables $T(t)$, $I(t)$, and $V(t)$ represent the density of uninfected cells, infected cells, and free virus particles at time t, respectively. The parameters s and d represent the production rate and natural mortality rate of target cells, respectively. The rate of virus infection is given by $\beta V(t)T(t)$, and δ represents the rate of death of infected cells. The release rate of virus from infected cells is p, and c is the rate at which progeny virus particles are removed. During antiviral therapy, the amount of virus produced by infected cells decreases to $(1-\varepsilon)pI(t)$, with efficacy ε where $0 < \varepsilon \leq 1$.

The model (2.1) does not include the process of intracellular viral replication, which means it ignores the multiscale characteristics between intracellular and intercellular viral infections. To separately quantify the antiviral effects of drugs on different viral replication processes, an extra equation is required to study the dynamics of the intracellular virus. Otherwise, all the antiviral effects of drugs on the processes of viral translation, processing, replication, assembly, transportation, and release are reflected in a single parameter ε.

The multiscale model has been proposed to more accurately describe the impact of different antiviral effects on the virus life cycle. In literature [11], an extra variable, R, is added to the model to represent the number of viral RNA in an infected cell. The dynamics of viral RNA in cells are determined by RNA production and degradation, as well as the loss of virus particles assembled or secreted into plasma. The multiscale model including intracellular viral RNA replication and extracellular viral infection is given by

$$\begin{cases} \dfrac{dT(t)}{dt} = s - \beta V(t)T(t) - dT(t), \\ \dfrac{\partial I(a,t)}{\partial a} + \dfrac{\partial I(a,t)}{\partial t} = -\delta(a)I(a,t), \\ I(0,t) = \beta V(t)T(t), \quad I(a,0) = I_0(a), \\ \dfrac{\partial R(a,t)}{\partial a} + \dfrac{\partial R(a,t)}{\partial t} = \alpha(a) - (\mu(a) + \rho(a))R(a,t), \\ R(0,t) = 1, \quad R(a,0) = R_0(a), \\ \dfrac{dV(t)}{dt} = \displaystyle\int_0^\infty \rho(a)R(a,t)I(a,t)da - cV(t), \end{cases} \tag{2.2}$$

where a represents the infection age of the infected cell, i.e., the time elapsed since HCV's entry into the cell. $I(a,t)$ and $R(a,t)$ represent the density of infected cells and intracellular viral RNA with the infection age of a at the time of t, respectively; The functions $\alpha(a)$, $\mu(a)$, $\rho(a)$ and $\delta(a)$ associated with infection age a represent intracellular viral RNA production, degradation, assembly/secretion rates, and mortality of infected cells, respectively. Assuming that cells are initially infected with a single virus, there is only one viral RNA in infected cells at the infection age of 0, denoted as $R(0,t) = 1$. The other parameters have the same biological meaning as the model (2.1). The model (2.2) was used to study the dynamics of HCV under DAAs treatment and obtain an approximate solution for the decline in viral load after treatment [11]. Other possible methods for incorporating intracellular viral dynamics into multiscale models were also discussed.

The error-prone nature of HCV RNA polymerase results in a high mismatch rate of the HCV RNA genome and a rapid replication rate of the HCV virus. These factors contribute to the high mutation rate of HCV RNA, which leads to the emergence of drug-resistant viruses [21]. In this paper, we investigate the prevalence of HCV variants and the evolution of resistance during DAAs treatment. We assume that sensitive infected cells produce sensitive viral strains and mutant variants at a certain rate (assuming a single mutation generates a certain degree of resistance), and we establish a multiscale age-structured HCV model that includes two strains (sensitive and resistant viral strains) of intracellular viral RNA replication and extracellular viral infection, given by the following system of differential equations:

$$\begin{cases} \dfrac{dT(t)}{dt} = s - dT(t) - \beta_s V_s(t)T(t) - \beta_r V_r(t)T(t), \\ \dfrac{\partial I_s(a,t)}{\partial a} + \dfrac{\partial I_s(a,t)}{\partial t} = -\delta(a)I_s(a,t), \\ \dfrac{\partial I_r(a,t)}{\partial a} + \dfrac{\partial I_r(a,t)}{\partial t} = -\delta(a)I_r(a,t), \\ \dfrac{\partial R_s(a,t)}{\partial a} + \dfrac{\partial R_s(a,t)}{\partial t} = (1-m)\alpha_s(a) - (\mu(a) + \rho(a))R_s(a,t), \\ \dfrac{\partial R_r(a,t)}{\partial a} + \dfrac{\partial R_r(a,t)}{\partial t} = m\alpha_s(a) - (\mu(a) + \rho(a))R_r(a,t), \\ \dfrac{\partial \widetilde{R}_r(a,t)}{\partial a} + \dfrac{\partial \widetilde{R}_r(a,t)}{\partial t} = \alpha_r(a) - (\mu(a) + \rho(a))\widetilde{R}_r(a,t), \\ \dfrac{dV_s(t)}{dt} = \displaystyle\int_0^\infty \rho(a)R_s(a,t)I_s(a,t)da - cV_s(t), \\ \dfrac{dV_r(t)}{dt} = \displaystyle\int_0^\infty \rho(a)R_r(a,t)I_s(a,t)da + \int_0^\infty \rho(a)\widetilde{R}_r(a,t)I_r(a,t)da - cV_r(t). \end{cases} \tag{2.3}$$

We assume the following initial conditions

$$\begin{aligned} &T(0) = T_0 \in \mathbb{R}_+,\ V_s(0) = V_{s0} \in \mathbb{R}_+,\ V_r(0) = V_{r0} \in \mathbb{R}_+,\ I_s(\cdot,0) = I_{s_0}(a) \in L^1_+(0,\infty), \\ &I_r(\cdot,0) = I_{r_0}(a) \in L^1_+(0,\infty),\ R_s(\cdot,0) = R_{s_0}(a) \in L^1_+(0,\infty),\ R_r(\cdot,0) = R_{r_0}(a) \in L^1_+(0,\infty), \\ &\widetilde{R}_r(\cdot,0) = \widetilde{R_{r_0}}(a) \in L^1_+(0,\infty), \end{aligned}$$

and boundary conditions

$$I_s(0,t) = \beta_s V_s(t)T(t),\quad I_r(0,t) = \beta_r V_r(t)T(t),\quad R_s(0,t) = 1,\quad R_r(0,t) = 0,\quad \widetilde{R}_r(0,t) = 1,$$

where $\mathbb{R}_+ = [0,\infty)$ and $L^1_+(0,\infty)$ is the positive cone of the Banach space $L^1(0,\infty)$. $V_s(t)$ and $V_r(t)$ represent the density of sensitive and resistant strains of virus at time t that invade uninfected cells at rates of $\beta_s V_s(t)T(t)$ and $\beta_r V_r(t)T(t)$, respectively, to produce the

corresponding infected cells. $I_s(a,t)$ and $I_r(a,t)$ represent the density of sensitive and resistant infected cells with the infection age a at time t, respectively. $R_s(a,t)$ and $\widetilde{R_r}(a,t)$ represent the density of intracellular drug-sensitive virus RNA and drug-resistant virus RNA at age a at time t, respectively, and $R_r(a,t)$ is the density of drug-resistant RNA produced by mutation of drug-sensitive infected cells at age a at time t. The functions $\alpha_s(a)$ and $\alpha_r(a)$ associated with the age of infection a represent the production of sensitive and resistant viral RNA, respectively. Considering a single mutation, we assume that virus RNA in drug-sensitive infected liver cells produces drug-resistant virus RNA with a probability m due to replication errors, which is about $10^{-4} - 10^{-5}$ per copied nucleotide. The other parameters have the same biological meaning as in model (2.2).

The multiscale model differs from the basic viral dynamic model (2.1) by distinguishing three antiviral effects of DAAs treatment: inhibiting the production of intracellular viral RNA, reducing the assembly/secretion of viruses in plasma, and enhancing the degradation rate of viral RNA. We assume that ε_s and ε_r represent the drug efficacies of DAAs in inhibiting viral RNA production for drug-sensitive and drug-resistant virus RNA, respectively. Similarly, η_s and η_r represent the drug efficacies of blocking the secretion of drug-sensitive virus and drug-resistant virus, respectively, and μ represents the degradation rate of virus RNA of the two strains. We increase μ by a factor κ to improve the degradation rate, where $0 \le \varepsilon_i \le 1, 0 \le \eta_i \le 1 (i = s,\ r)$ and $\kappa \ge 1$ refer to the effectiveness of therapy on different processes in the virus life cycle. The complete model combines intracellular and extracellular virus dynamics of two strains during treatment, and is given by

$$
\begin{cases}
\dfrac{dT(t)}{dt} = s - dT(t) - \beta_s V_s(t)T(t) - \beta_r V_r(t)T(t), \\
\dfrac{\partial I_s(a,t)}{\partial a} + \dfrac{\partial I_s(a,t)}{\partial t} = -\delta(a) I_s(a,t), \\
I_s(0,t) = \beta_s V_s(t)T(t), \quad I_s(a,0) = \bar{I}_s(a), \\
\dfrac{\partial I_r(a,t)}{\partial a} + \dfrac{\partial I_r(a,t)}{\partial t} = -\delta(a) I_r(a,t), \\
I_r(0,t) = \beta_r V_r(t)T(t), \quad I_r(a,0) = \bar{I}_r(a), \\
\dfrac{\partial R_s(a,t)}{\partial a} + \dfrac{\partial R_s(a,t)}{\partial t} = (1-m)(1-\varepsilon_s)\alpha_s(a) - (\kappa\mu(a) + (1-\eta_s)\rho(a)) R_s(a,t), \\
R_s(0,t) = 1, \quad R_s(a,0) = \bar{R}_s(a), \\
\dfrac{\partial R_r(a,t)}{\partial a} + \dfrac{\partial R_r(a,t)}{\partial t} = m(1-\varepsilon_s)\alpha_s(a) - (\kappa\mu(a) + (1-\eta_r)\rho(a)) R_r(a,t), \\
R_r(0,t) = 0, \quad R_r(a,0) = \bar{R}_r(a), \\
\dfrac{\partial \widetilde{R_r}(a,t)}{\partial a} + \dfrac{\partial \widetilde{R_r}(a,t)}{\partial t} = (1-\varepsilon_r)\alpha_r(a) - (\kappa\mu(a) + (1-\eta_r)\rho(a)) \widetilde{R_r}(a,t), \\
\widetilde{R_r}(0,t) = 1, \quad \widetilde{R_r}(a,0) = \overline{\widetilde{R_r}}(a), \\
\dfrac{dV_s(t)}{dt} = (1-\eta_s) \displaystyle\int_0^\infty \rho(a) R_s(a,t) I_s(a,t) da - cV_s(t), \\
\dfrac{dV_r(t)}{dt} = (1-\eta_r) \displaystyle\int_0^\infty \rho(a) R_r(a,t) I_s(a,t) da \\
\qquad\qquad + (1-\eta_r) \displaystyle\int_0^\infty \rho(a) \widetilde{R_r}(a,t) I_r(a,t) da - cV_r(t),
\end{cases}
\tag{2.4}
$$

where $t = 0$ is the time at which treatment is initiated, $\bar{I}_s(a)$ and $\bar{I}_r(a)$ are the steady-state distributions of infected cells with drug-sensitive and drug-resistant, respectively, before therapy. $\bar{R}_s(a)$, $\overline{\widetilde{R_r}}(a)$ and $\bar{R}_r(a)$ are the steady-state distributions of intracellular drug-sensitive virus RNA, drug-resistant virus RNA and drug-resistant RNA produced by mutation of drug-sensitive infected cells, respectively, before therapy. The schematic diagram of the model (2.4) is shown in Fig. 1.

In order to study the dynamic properties of the model (2.3), it is assumed that the following holds:

(A_1) $\delta(\cdot)$, $\alpha_s(\cdot)$, $\alpha_r(\cdot)$, $\mu(\cdot)$, $\rho(\cdot) \in L^\infty_+(0,\infty)$ are uniformly continuous and bounded, where $L^\infty_+(0,\infty)$ is the positive cone of the Banach space $L^\infty(0,\infty)$. $\rho(a)$ cannot be a zero parameter. Otherwise, virus particles will not be produced.

(A_2) Assuming $I_s(0,0) = I_{s0}(0) = \beta_s V_{s0} T_0$, $I_r(0,0) = I_{r0}(0) = \beta_r V_{r0} T_0$, $R_s(0,0) = R_{s0}(0) = 1$, $R_r(0,0) = R_{r0}(0) = 0$, $\widetilde{R_r}(0,0) = \widetilde{R_{r0}}(0) = 1$.

The state space of model (2.3) is

$$X_+ = \mathbb{R}_+ \times L^1_+(0,\infty) \times L^1_+(0,\infty) \times L^1_+(0,\infty) \times L^1_+(0,\infty) \times \mathbb{R}_+ \times \mathbb{R}_+.$$

Obviously, X_+ is a nonnegative cone on the Banach space $\mathbb{R} \times L^1(0,\infty) \times L^1(0,\infty) \times L^1(0,\infty) \times L^1(0,\infty) \times \mathbb{R} \times \mathbb{R}$.

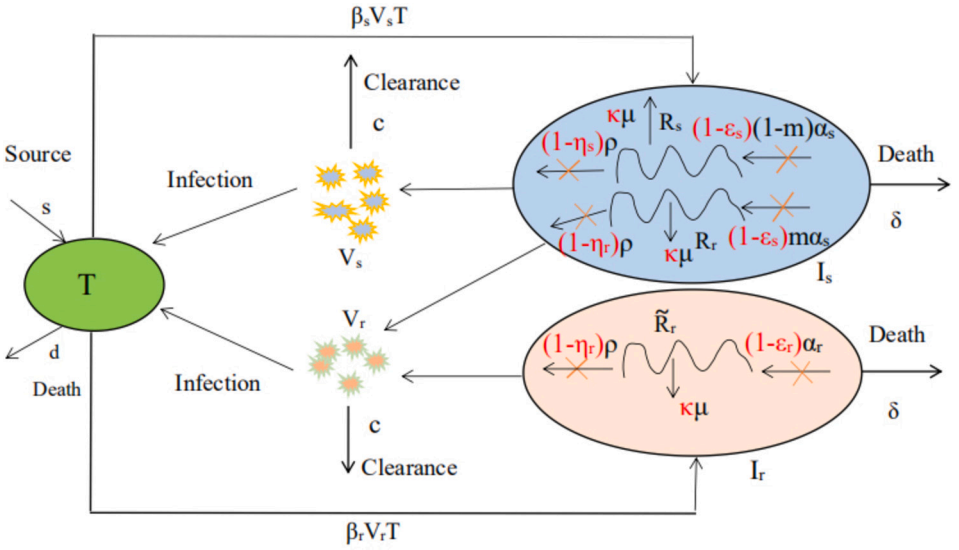

Fig. 1. Schematic diagram of model (2.4).

Denote

$$\|(T, I_s, I_r, R_s, R_r, \widetilde{R_r}, V_s, V_r)\| = |T| + \|I_s\|_1 + \|I_r\|_1 + \|R_s\|_1 + \|R_r\|_1 + \|\widetilde{R_r}\|_1 + |V_s| + |V_r|,$$

where $(T, I_s, I_r, R_s, R_r, \widetilde{R_r}, V_s, V_r) \in \mathbb{R} \times L^1(0,\infty) \times L^1(0,\infty) \times L^1(0,\infty) \times L^1(0,\infty) \times \mathbb{R} \times \mathbb{R}$. It follows from [22,23] that model (2.3) has a unique continuous solution in X_+ if the initial value $(T_0, I_{s0}, I_{r0}, R_{s0}, R_{r0}, \widetilde{R_{r0}}, V_{s0}, V_{r0}) \in X_+$ satisfies (A_2). It implies that a solution semiflow $\Phi : \mathbb{R}_+ \times X_+ \to X_+$ given by

$$\Phi(t, (T_0, I_{s0}, I_{r0}, R_{s0}, R_{r0}, \widetilde{R_{r0}}, V_{s0}, V_{r0})) = (T(t), I_s(\cdot,t), I_r(\cdot,t), R_s(\cdot,t), R_r(\cdot,t), \widetilde{R_r}(\cdot,t), V_s(t), V_r(t)),$$

where $t \in \mathbb{R}_+$ and $(T(t), I_s(a,t), I_r(a,t), R_s(a,t), R_r(a,t), \widetilde{R_r}(a,t), V_s(t), V_r(t))$, is the unique solution of (2.3) through the initial value $(T_0, I_{s0}, I_{r0}, R_{s0}, R_{r0}, \widetilde{R_{r0}}, V_{s0}, V_{r0}) \in X_+$.

Let

$$G_1(t) = T(t) + \int_0^\infty I_s(a,t)da + \int_0^\infty I_r(a,t)da,$$

$$G_2(t) = \int_0^\infty R_s(a,t)da + \int_0^\infty R_r(a,t)da + \int_0^\infty \widetilde{R_r}(a,t)da,$$

$$G_3(t) = V_s(t) + V_r(t).$$

It follows from (2.3) that

$$\begin{aligned}\frac{dG_1(t)}{dt} &\le s - dT(t) - \int_0^\infty \delta(a) I_s(a,t)da - \int_0^\infty \delta(a) I_r(a,t)da \\ &\le s - m_1 G_1(t),\end{aligned}$$

where $m_1 = \min\{d, n_0\}$, $n_0 = \inf\limits_{a\in(0,\infty)}\{\delta(a)\}$. It implies that $\limsup\limits_{t\to\infty} G_1(t) \le \frac{s}{m_1}$.

Similarly,

$$\begin{aligned}\frac{dG_2(t)}{dt} &\le 2 + \|\alpha_s\|^\infty + \|\alpha_r\|^\infty - \int_0^\infty (\mu(a)+\rho(a)) R_s(a,t)da - \int_0^\infty (\mu(a)+\rho(a)) R_r(a,t)da \\ &\quad - \int_0^\infty (\mu(a)+\rho(a))\widetilde{R_r}(a,t)da \\ &\le 2 + \|\alpha_s\|^\infty + \|\alpha_r\|^\infty - m_2 G_2(t),\end{aligned}$$

where $m_2 = \inf\limits_{a\in(0,\infty)}\{\mu(a)+\rho(a)\}$. We have $\limsup\limits_{t\to\infty} G_2(t) \le \frac{2+\|\alpha_s\|^\infty+\|\alpha_r\|^\infty}{m_2}$.

Next, it follows from

$$\frac{dG_3(t)}{dt} \le 3\|\rho\|^\infty \frac{2+\|\alpha_s\|^\infty+\|\alpha_r\|^\infty}{m_2}\frac{s}{m_1} - cG_3(t)$$

that $\limsup_{t\to\infty} G_3(t) \le \frac{3\|\rho\|^\infty s}{cm_1}\frac{2+\|\alpha_s\|^\infty+\|\alpha_r\|^\infty}{m_2}$.

To sum up, the set

$$\Omega = \left\{ (T, I_s, I_r, R_s, R_r, \widetilde{R_r}, V_s, V_r) \in X_+ | T + \|I_s\| + \|I_r\| \le \frac{s}{m_1}, \right.$$
$$\left. \|R_s\| + \|R_r\| + \|\widetilde{R_r}\| \le \frac{2+\|\alpha_s\|^\infty+\|\alpha_r\|^\infty}{m_2},\ V_s + V_r \le \frac{3\|\rho\|^\infty s}{cm_1}\frac{2+\|\alpha_s\|^\infty+\|\alpha_r\|^\infty}{m_2} \right\}$$

is positively invariant with respect to (2.3).

3. Model analysis

In this section, we study the steady states of model (2.3) and analyze their stability. Model (2.4) with treatment can be analyzed similarly.

Let

$$\omega(a) = e^{-\int_0^a \delta(\tau)d\tau}, \qquad \pi(a) = e^{-\int_0^a [\rho(\tau)+\mu(\tau)]d\tau},$$

where $\omega(a)$ and $\pi(a)$ represent the survival probability of an infected cell and an intracellular viral RNA for the infected age a, respectively. The densities of infected cells of two strains of age a in the stable state are

$$\bar{I}_s(a) = I_s(0)\omega(a) = \beta_s \bar{V}_s \bar{T}\omega(a), \qquad \bar{I}_r(a) = I_r(0)\omega(a) = \beta_r \bar{V}_r \bar{T}\omega(a), \tag{3.1}$$

where $\bar{V}_s$ and $\bar{V}_r$ are the steady state viral loads with drug-sensitive and drug-resistant density, respectively. $\bar{T}$ represents the density of target cells at the steady state. We assume that a cell is initially infected with a virus particle. Therefore, when an infected cell is at age $a = 0$, there is only one corresponding viral RNA, i.e., $R_s(0) = 1,\ R_r(0) = 0,\ \widetilde{R_r}(0) = 1$. The steady states of virus RNA level of the two strains of age a are

$$\begin{aligned} &\bar{R}_s(a) = \pi(a) + (1-m)\int_0^a \alpha_s(\tau)\frac{\pi(a)}{\pi(\tau)}d\tau, \quad \bar{R}_r(a) = m\int_0^a \alpha_s(\tau)\frac{\pi(a)}{\pi(\tau)}d\tau, \\ &\overline{\widetilde{R_r}}(a) = \pi(a) + \int_0^a \alpha_r(\tau)\frac{\pi(a)}{\pi(\tau)}d\tau. \end{aligned} \tag{3.2}$$

We substitute the steady states $\bar{I}_s(a),\ \bar{I}_r(a)$ and $\bar{R}_s(a),\ \bar{R}_r(a),\ \overline{\widetilde{R_r}}(a)$ in (3.1) and (3.2) into $V_s(t)$ and $V_r(t)$ in (2.3), and obtain

$$\int_0^\infty \rho(a)\bar{R}_s(a)\beta_s\bar{V}_s\bar{T}\omega(a)da = c\bar{V}_s,$$
$$\int_0^\infty \rho(a)\bar{R}_r(a)\beta_s\bar{V}_s\bar{T}\omega(a)da + \int_0^\infty \rho(a)\overline{\widetilde{R_r}}(a)\beta_r\bar{V}_r\bar{T}\omega(a)da = c\bar{V}_r.$$

Let $N_s = \int_0^\infty \rho(a)\bar{R}_s(a)\omega(a)da,\ N_r = \int_0^\infty \rho(a)\bar{R}_r(a)\omega(a)da,\ \widetilde{N_r} = \int_0^\infty \rho(a)\overline{\widetilde{R_r}}(a)\omega(a)da$. N_s represents the total number of virus particles (V_s) produced by a drug-sensitive infected cell (I_s) without mutation in its lifetime. N_r represents the total number of virus particles (V_r) produced by a drug-sensitive infected cell (I_s) with mutation in its lifetime and $\widetilde{N_r}$ represents the total number of virus particles (V_r) produced by a drug-resistant infected cell (I_r) in its lifetime. Based on the above discussion, it is easy to see that $\bar{T} = \frac{c}{\beta_s N_s}$ and

$$\beta_s\bar{V}_s\bar{T}N_r + \beta_r\bar{V}_r\bar{T}\widetilde{N_r} = c\bar{V}_r. \tag{3.3}$$

From the first equation of model (2.3) and (3.3), we obtain the viral loads of the two strains in the steady state

$$\bar{V}_s = \frac{(\beta_s N_s - \beta_r\widetilde{N_r})(s\beta_s N_s - dc)}{\beta_s c(\beta_s N_s - \beta_r\widetilde{N_r} + \beta_r N_r)}, \qquad \bar{V}_r = \frac{(s\beta_s N_s - dc)N_r}{c(\beta_s N_s - \beta_r\widetilde{N_r} + \beta_r N_r)}.$$

Obviously, $\bar{V}_s = \frac{\beta_s N_s - \beta_r\widetilde{N_r}}{\beta_s N_r}\bar{V}_r$. Plugging the steady states $\bar{T},\ \bar{V}_s$, and $\bar{V}_r$ into (3.1), we get

$$\bar{I}_s(a) = \frac{(\beta_s N_s - \beta_r\widetilde{N_r})(s\beta_s N_s - dc)}{\beta_s N_s(\beta_s N_s - \beta_r\widetilde{N_r} + \beta_r N_r)}\omega(a), \quad \bar{I}_r(a) = \frac{\beta_r N_r(s\beta_s N_s - dc)}{\beta_s N_s(\beta_s N_s - \beta_r\widetilde{N_r} + \beta_r N_r)}\omega(a).$$

Denote

$$R_1 = \frac{\beta_r s}{dc}\widetilde{N_r}, \quad R_2 = \frac{\beta_s s}{dc}N_s.$$

R_1 is the basic reproduction number of the drug-resistant strain of model (2.3) and represents the number of next-generation viruses with drug resistance produced by infected cells in their life cycle. R_2 is the basic reproduction number of the drug-sensitive strain of model (2.3) and represents the number of next-generation viruses produced by drug-resistant infected cells in their life cycle.

The conditions for the existence of three steady states of model (2.2) are given below:

(i) The infection-free steady state is $E_0 = (s/d, 0, 0, \bar{R}_s(a), \bar{R}_r(a), \overline{\widetilde{R_r}}(a), 0, 0)$.

(ii) If $R_1 > 1$, then there is the boundary steady state: $E_1 = (\bar{T}_1, 0, \bar{I}_{r_1}, \bar{R}_s(a), \bar{R}_r(a), \overline{\widetilde{R_r}}(a), 0, \bar{V}_{r_1})$, where $\bar{T}_1 = c/\beta_r\widetilde{N_r}$, $\bar{I}_{r_1} = (s\beta_r\widetilde{N_r} - dc)\omega(a)/\beta_r\widetilde{N_r}$, $\bar{V}_{r_1} = (s\beta_r\widetilde{N_r} - dc)/\beta_r c$.

(iii) If $R_2 > 1$ and $R_2 > R_1$, then there is a coexistence steady state:

$E_2 = (\bar{T}, \bar{I}_s(a), \bar{I}_r(a), \bar{R}_s(a), \bar{R}_r(a), \overline{\widetilde{R_r}}(a), \bar{V}_s, \bar{V}_r)$.

We use the method of characteristic lines to find the complete solutions of $R_s(a,t)$, $R_r(a,t)$, $\widetilde{R_r}(a,t)$, $I_s(a,t)$, and $I_r(a,t)$. Assuming that the characteristic curve is $t - a =$ constant and they intersect the age axis by $(a_0, 0)$ and the time axis by $(0, t_0)$, where $a_0 \geq 0$, $t_0 \geq 0$.

When $a \geq t$, the following describes the characteristic curve with parametric equation $t = \tau$, $a = \tau + a_0$, where τ is a free parameter. When $\tau \in (0,t)$, $a(\tau) \in (a_0, a)$, $t(\tau) \in (0,t)$, the variable follows the characteristic curves and we obtain

$$\frac{dR_s(a(\tau),t(\tau))}{d\tau} = \frac{\partial R_s}{\partial t}\frac{dt}{d\tau} + \frac{\partial R_s}{\partial a}\frac{da}{d\tau} = (1-m)\alpha_s(a(\tau)) - [\rho(a(\tau)) + \mu(a(\tau))]R_s(a(\tau),t(\tau)). \tag{3.4}$$

This is an ordinary differential equation. Using the constant variation method, we have

$$\begin{aligned} R_s(a,t) &= R_s(a_0,0)e^{-\int_0^t[\rho(a(\tau))+\mu(a(\tau))]d\tau} \\ &\quad + e^{-\int_0^t[\rho(a(\tau))+\mu(a(\tau))]d\tau}\int_0^t (1-m)\alpha_s(a(u))e^{-\int_0^u[\rho(a(u))+\mu(a(u))]d\tau}du. \end{aligned}$$

Noting that

$$\int_0^t [\rho(a(\tau)) + \mu(a(\tau))]d\tau = \int_{a_0}^a [\rho(\varsigma) + \mu(\varsigma)]d\varsigma$$

and

$$e^{-\int_0^t[\rho(a(\tau))+\mu(a(\tau))]d\tau} = e^{-\int_{a_0}^a[\rho(\varsigma)+\mu(\varsigma)]d\varsigma} = \frac{\pi(a)}{\pi(a_0)},$$

we obtain

$$\begin{aligned} \int_0^t \alpha_s(a(u))e^{\int_0^u[\rho(a(\tau))+\mu(a(\tau))]d\tau}du &= \int_0^t \alpha_s(a(u))e^{\int_{a_0}^{a_0+u}[\rho(\eta)+\mu(\eta)]d\eta}du \\ &= \int_{a_0}^a \alpha_s(\varsigma)e^{\int_{a_0}^{\varsigma}[\rho(\eta)+\mu(\eta)]d\eta}d\varsigma \\ &= \int_{a_0}^a \alpha_s(\varsigma)\frac{\pi(a_0)}{\pi(\varsigma)}d\varsigma. \end{aligned}$$

Therefore, when $a \geq t$, we have

$$\begin{aligned} R_s(a,t) &= R_s(a_0,0)\frac{\pi(a)}{\pi(a_0)} + \frac{\pi(a)}{\pi(a_0)}(1-m)\int_{a_0}^a \alpha_s(\varsigma)\frac{\pi(a_0)}{\pi(\varsigma)}d\varsigma \\ &= R_{s_0}(a-t)\frac{\pi(a)}{\pi(a-t)} + \int_0^t \frac{\pi(a)}{\pi(a-u)}(1-m)\alpha_s(a-u)du. \end{aligned}$$

When $a < t$, the following describes the characteristic curve with parametric equation $t = \tau$, $a = \tau - t_0$, where τ is a free parameter. When $\tau \in (t_0, t)$, $a(\tau) \in (0, a)$, $t(\tau) \in (t_0, t)$, the variable follows the characteristic curves and we obtain the same ordinary differential equation as (3.4), and use the ordinary differential variation method to obtain the following

$$\begin{aligned} R_s(a,t) &= R_s(0,t_0)e^{-\int_{t_0}^t[\rho(a(\tau))+\mu(a(\tau))]d\tau} \\ &\quad + e^{-\int_{t_0}^t[\rho(a(\tau))+\mu(a(\tau))]d\tau}\int_{t_0}^t (1-m)\alpha_s(a(u))e^{-\int_{t_0}^u[\rho(a(\tau))+\mu(a(\tau))]d\tau}du. \end{aligned}$$

From

$$e^{-\int_{t_0}^{t}[\rho(a(\tau))+\mu(a(\tau))]d\tau} = e^{-\int_{0}^{a}[\rho(\varsigma)+\mu(\varsigma)]d\varsigma} = \pi(a),$$

we have

$$\begin{aligned}\int_{t_0}^{t}\alpha_s(a(u))e^{\int_{t_0}^{u}[\rho(a(\tau))+\mu(a(\tau))]d\tau}du &= \int_{t_0}^{t}\alpha_s(a(u))e^{\int_{0}^{u-t_0}[\rho(\eta)+\mu(\eta)]d\eta}du\\ &= \int_{t_0}^{t}\frac{\alpha_s(u-t_0)}{\pi(u-t_0)}du = \int_{0}^{t-t_0}\frac{\alpha_s(\xi)}{\pi(\xi)}d\xi = \int_{0}^{a}\frac{\alpha_s(\xi)}{\pi(\xi)}d\xi.\end{aligned}$$

Thus, when $a < t$, we get

$$\begin{aligned}R_s(a,t) &= R_s(0,t-a)\pi(a) + \pi(a)\int_0^a (1-m)\frac{\alpha_s(u)}{\pi(u)}du\\ &= \pi(a) + \int_0^a (1-m)\frac{\pi(a)}{\pi(u)}\alpha_s(u)du.\end{aligned}$$

The complete solution of $R_s(a,t)$ is as follows

$$R_s(a,t) = \begin{cases}\pi(a) + \int_0^a (1-m)\frac{\pi(a)}{\pi(u)}\alpha_s(u)du, & a < t,\\ R_{s_0}(a-t)\frac{\pi(a)}{\pi(a-t)} + \int_0^t \frac{\pi(a)}{\pi(a-u)}(1-m)\alpha_s(a-u)du, & a \geq t.\end{cases} \tag{3.5}$$

We use a similar method to obtain the complete solution of the other variables before treatment, given by

$$R_r(a,t) = \begin{cases}\int_0^a m\frac{\pi(a)}{\pi(u)}\alpha_s(u)du, & a < t,\\ R_{r_0}(a-t)\frac{\pi(a)}{\pi(a-t)} + \int_0^t \frac{\pi(a)}{\pi(a-u)}m\alpha_s(a-u)du, & a \geq t,\end{cases} \tag{3.6}$$

$$\widetilde{R_r}(a,t) = \begin{cases}\pi(a) + \int_0^a \frac{\pi(a)}{\pi(u)}\alpha_r(u)du, & a < t,\\ \widetilde{R_{r_0}}(a-t)\frac{\pi(a)}{\pi(a-t)} + \int_0^t \frac{\pi(a)}{\pi(a-u)}\alpha_r(a-u)du, & a \geq t,\end{cases} \tag{3.7}$$

$$I_s(a,t) = \begin{cases}\beta_s V_s(t-a)T(t-a)\omega(a), & a < t,\\ I_{s_0}(a-t)\frac{\omega(a)}{\omega(a-t)}, & a \geq t,\end{cases} \tag{3.8}$$

and

$$I_r(a,t) = \begin{cases}\beta_r V_r(t-a)T(t-a)\omega(a), & a < t,\\ I_{r_0}(a-t)\frac{\omega(a)}{\omega(a-t)}, & a \geq t.\end{cases} \tag{3.9}$$

Substituting the expressions of (3.5)-(3.9) into model (2.3), we obtain

$$\begin{cases}\frac{dT(t)}{dt} = s - dT(t) - K_s(t) - K_r(t),\\ \frac{dV_s(t)}{dt} = \int_0^t K_s(t-a)Q_s(a)da - cV_s(t) + F_s(t),\\ \frac{dV_r(t)}{dt} = \int_0^t K_s(t-a)Q_r(a)da + \int_0^t K_r(t-a)Q_{\bar{r}}(a)da - cV_r(t) + F_{sr}(t) + F_r(t),\end{cases} \tag{3.10}$$

where

$$K_s(t)=\beta_s V_s(t)T(t),\quad K_r(t)=\beta_r V_r(t)T(t),\quad Q_s(a)=\rho(a)\bar{R}_s(a)\omega(a),$$
$$Q_r(a)=\rho(a)\bar{R}_r(a)\omega(a),\quad Q_{\tilde{r}}(a)=\rho(a)\overline{\widetilde{R}_r}(a)\omega(a),$$
$$F_s(t)=\int_t^\infty \rho(a)\left[R_{s_0}(a-t)\frac{\pi(a)}{\pi(a-t)}+\int_0^t \frac{\pi(a)}{\pi(a-u)}(1-m)\alpha_s(a-u)du\right]I_{s_0}(a-t)\frac{\omega(a)}{\omega(a-t)}da,$$
$$F_{sr}(t)=\int_t^\infty \rho(a)\left[R_{r_0}(a-t)\frac{\pi(a)}{\pi(a-t)}+\int_0^t \frac{\pi(a)}{\pi(a-u)}m\alpha_s(a-u)du\right]I_{s_0}(a-t)\frac{\omega(a)}{\omega(a-t)}da,$$
$$F_r(t)=\int_t^\infty \rho(a)\left[\widetilde{R}_{r_0}(a-t)\frac{\pi(a)}{\pi(a-t)}+\int_0^t \frac{\pi(a)}{\pi(a-u)}\alpha_r(a-u)du\right]I_{r_0}(a-t)\frac{\omega(a)}{\omega(a-t)}da.$$

It is clear that $F_s(t)\to 0$, $F_{sr}(t)\to 0$, and $F_r(t)\to 0$ as $t\to\infty$. We integrate the above equations in model (3.10) to obtain

$$\begin{aligned}
T(t)=&T_0e^{-dt}+\int_0^t[s-K_s(u)-K_r(u)]e^{-d(t-u)}du,\\
V_s(t)=&V_{s_0}e^{-ct}+\int_0^t\left[\int_0^u K_s(u-a)Q_s(a)da+F_s(u)\right]e^{-c(t-u)}du,\\
V_r(t)=&V_{r_0}e^{-ct}+\int_0^t\left[\int_0^u K_s(u-a)Q_r(a)da\right.\\
&\left.+\int_0^u K_r(u-a)Q_{\tilde{r}}(a)da+F_{sr}(u)+F_r(u)\right]e^{-c(t-u)}du.
\end{aligned}\tag{3.11}$$

By changing the integration order of $V_s(t)$ and $V_r(t)$ in (3.11), we get

$$\begin{aligned}
\int_0^t e^{-c(t-u)}\int_0^u K_s(u-a)Q_s(a)dadu&=\int_0^t e^{-c(t-u)}\int_0^u K_s(\xi)Q_s(u-\xi)d\xi du\\
&=\int_0^t K_s(\xi)\int_\xi^t e^{-c(t-u)}Q_s(u-\xi)dud\xi\\
&=\int_0^t K_s(\xi)e^{-c(t-\xi)}\int_0^{t-\xi}e^{c\eta}Q_s(\eta)d\eta d\xi\\
&=\int_0^t K_s(\xi)H_s(t-\xi)d\xi,
\end{aligned}$$

where $H_s(t)=e^{-ct}\int_0^t e^{c\eta}Q_s(\eta)d\eta$.

Similarly, we have

$$\int_0^t e^{-c(t-u)}\int_0^u K_s(u-a)Q_r(a)dadu=\int_0^t K_s(\xi)H_r(t-\xi)d\xi,$$
$$\int_0^t e^{-c(t-u)}\int_0^u K_r(u-a)Q_{\tilde{r}}(a)dadu=\int_0^t K_r(\xi)H_{\tilde{r}}(t-\xi)d\xi,$$

where $H_r(t)=e^{-ct}\int_0^t e^{c\eta}Q_r(\eta)d\eta$, $H_{\tilde{r}}(t)=e^{-ct}\int_0^t e^{c\eta}Q_{\tilde{r}}(\eta)d\eta$. Thus, model (3.11) can be changed to

$$\begin{aligned}
T(t)&=\int_0^t[s-\beta_s V_s(u)T(u)-\beta_r V_r(u)T(u)]e^{-d(t-u)}du+F_1(t),\\
V_s(t)&=\int_0^t\beta_s V_s(u)T(u)H_s(t-u)du+F_2(t),
\end{aligned}\tag{3.12}$$

$$V_r(t) = \int_0^t \beta_s V_s(u)T(u)H_r(t-u)du + \int_0^t \beta_r V_r(u)T(u)H_{\bar{r}}(t-u)du + F_3(t),$$

where $F_1(t) = T_0 e^{-dt},\ F_2(t) = V_{s_0}e^{-ct} + \int_0^t F_s(u)e^{-c(t-u)}du,\ F_3(t) = V_{r_0}e^{-ct} + \int_0^t [F_{sr}(u) + F_r(u)]e^{-c(t-u)}du$. The above-converted model (3.12) can be expressed in a general form. Let $x(t) = (T(t), V_s(t), V_r(t))^{\mathrm{T}}$, where T represents the transposition of the vector. Model (3.12) can be rewritten as

$$x(t) = \int_0^t h(t-u)g(x(u))du + f(t), \tag{3.13}$$

where

$$h(t) = \begin{pmatrix} se^{-dt} & -e^{-dt} & -e^{-dt} \\ 0 & H_s(t) & 0 \\ 0 & H_r(t) & H_{\bar{r}}(t) \end{pmatrix},\ g(t) = \begin{pmatrix} 1 \\ \beta_s V_s(t)T(t) \\ \beta_r V_r(t)T(t) \end{pmatrix},\ f(t) = \begin{pmatrix} F_1(t) \\ F_2(t) \\ F_3(t) \end{pmatrix}.$$

This forms a Volterra integral equation model equivalent to model (2.3), where $h(t)$ is a locally integrable function and $g(t)$ and $f(t)$ are continuous functions, i.e., $h \in L^1_{loc}([0,\infty);\ \mathbf{R}^{3\times 3}),\ g \in C(\mathbf{R}^3, \mathbf{R}^3),\ f \in C([0,\infty); \mathbf{R}^3)$. It follows from Theorem 1.1 in Gripenberg et al. [24] that model (3.13) has a unique solution and the solution is continuously dependent on the initial conditions. All solutions of model (2.3) are non-negative under positive initial values. Model (3.10) is also equivalent to model (2.3). Assume that there exists a $t_0 > 0$ such that $V_s(t_0) = 0,\ T(t) > 0,\ V_s(t) > 0$ for $0 \le t < t_0$. Noting that $K_s(t) = \beta_s V_s(t)T(t) > 0$ for $0 \le t < t_0$, and according to the $V_s(t)$ formula of model (3.10), we get

$$\frac{dV_s(t_0)}{dt} = \int_0^{t_0} K_s(t_0 - a)Q_s(a)da + F_s(t_0) > 0.$$

Thus, $V_s(t) \ge 0$ for all $t \ge 0$. Similarly, we conclude that $T(t) \ge 0,\ V_r(t) \ge 0$ for all $t \ge 0$ and for all positive initial data.

It follows from [24] that if any equilibrium of model (3.10) exists, it must be the constant solution of the limiting model related to (3.10), expressed by the following

$$\begin{cases} \dfrac{dT(t)}{dt} = s - dT(t) - \beta_s V_s(t)T(t) - \beta_r V_r(t)T(t), \\ \dfrac{dV_s(t)}{dt} = \displaystyle\int_0^\infty \beta_s V_s(t-a)T(t-a)\rho(a)\omega(a)\bar{R}_s(a)da - cV_s(t), \\ \dfrac{dV_r(t)}{dt} = \displaystyle\int_0^\infty \beta_s V_s(t-a)T(t-a)\rho(a)\omega(a)\bar{R}_r(a)da \\ \qquad\quad + \displaystyle\int_0^\infty \beta_r V_r(t-a)T(t-a)\rho(a)\omega(a)\overline{\widetilde{R}_r}(a)da - cV_r(t), \end{cases} \tag{3.14}$$

where $\bar{R}_s(a),\ \bar{R}_r(a),\ \overline{\widetilde{R}_r}(a)$ are given in (3.2). We have the following results on the infection-free steady state $E_0^* = (\bar{T}_0, 0, 0) = (s/d, 0, 0)$ and infection steady state of the limiting model (3.14).

(i) If $R_1 > 1$, then the following boundary steady state exists:

$$E_1^* = (\bar{T}_1,\ 0,\ \bar{V}_{r_1}) = \left(\frac{c}{\beta_r \widetilde{N}_r},\ 0,\ \frac{d}{\beta_r}(R_1 - 1)\right).$$

(ii) If $R_2 > 1$ and $R_2 > R_1$, then the following coexistence steady state exists:

$$E_2^* = (\bar{T},\ \bar{V}_s,\ \bar{V}_r) = \left(\frac{c}{\beta_s N_s},\ \frac{(\beta_s N_s - \beta_r \widetilde{N}_r)d}{\beta_s(\beta_s N_s - \beta_r \widetilde{N}_r + \beta_r N_r)}(R_2 - 1),\ \frac{N_r d}{(\beta_s N_s - \beta_r \widetilde{N}_r + \beta_r N_r)}(R_2 - 1)\right).$$

Next, we use the same method of finite ODE to study the infinite-dimensional model. This method has been used to study other age-structured models [25,26]. Fig. 2 shows the conditions under which the steady state of model (3.14) exists. We will use the equivalent model (3.14) of model (2.3) to study its stability. Linearizing the model (3.14) about the steady state $\tilde{E} = (\tilde{T}, \tilde{V}_s, \tilde{V}_r)$, we get the corresponding characteristic equation

$$\Delta(\tilde{E}) = \begin{vmatrix} -d - \beta_s \tilde{V}_s - \beta_r \tilde{V}_r - \lambda & -\beta_s \tilde{T} & -\beta_r \tilde{T} \\ \beta_s \tilde{V}_s n_1 & \beta_s \tilde{T} n_1 - c - \lambda & 0 \\ \beta_s \tilde{V}_s n_2 + \beta_r \tilde{V}_r n_3 & \beta_s \tilde{T} n_2 & \beta_r \tilde{T} n_3 - c - \lambda \end{vmatrix} = 0, \tag{3.15}$$

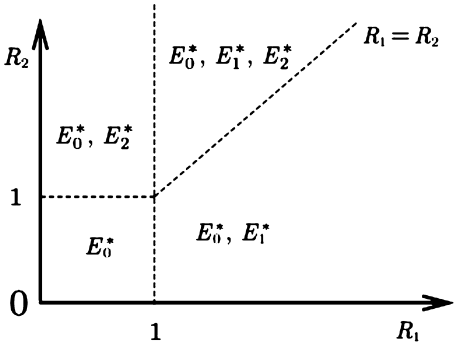

Fig. 2. Schematic diagram of the existence of the steady state of model (3.14) on the R_1-R_2 plane.

where $n_1 = \int_0^\infty \rho(a)\omega(a)\bar{R}_s(a)e^{-\lambda a}\mathrm{d}a$, $n_2 = \int_0^\infty \rho(a)\omega(a)\bar{R}_r(a)e^{-\lambda a}\mathrm{d}a$, $n_3 = \int_0^\infty \rho(a)\omega(a)\overline{\widetilde{R}_r}(a)e^{-\lambda a}\mathrm{d}a$, and λ denotes the eigenvalue of the linearized model.

Theorem 3.1. *The infection-free steady state E_0^* of model (3.14) is locally asymptotically stable if $R_1 < 1$ and $R_2 < 1$, and it is unstable when $R_1 > 1$ or $R_2 > 1$.*

Proof. We substitute $\tilde{E} = E_0^*$ into the above characteristic equation (3.15) to obtain the following characteristic polynomial

$$\left(\beta_s \bar{T}_0 \int_0^\infty \rho(a)\omega(a)\bar{R}_s(a)e^{-\lambda a}da - c - \lambda\right) \times \left(\beta_r \bar{T}_0 \int_0^\infty \rho(a)\omega(a)\overline{\widetilde{R}_r}(a)e^{-\lambda a}da - c - \lambda\right) \times (d+\lambda) = 0. \tag{3.16}$$

The characteristic polynomial (3.16) has one negative solution $-d$. Other eigenvalues are determined by the following equations

$$\begin{aligned} &\frac{\lambda}{c} + 1 = \frac{\beta_s s}{dc} \int_0^\infty \rho(a)\omega(a)\overline{\widetilde{R}_r}(a)e^{-\lambda a}da = R_1 \frac{\int_0^\infty \rho(a)\omega(a)\overline{\widetilde{R}_r}(a)e^{-\lambda a}da}{\widetilde{N_r}}, \\ &\frac{\lambda}{c} + 1 = R_2 \frac{\int_0^\infty \rho(a)\omega(a)\bar{R}_s(a)e^{-\lambda a}da}{N_s}. \end{aligned} \tag{3.17}$$

For all complex roots λ with non-negative real parts, we have

$$\left|\int_0^\infty \rho(a)\omega(a)\overline{\widetilde{R}_r}(a)e^{-\lambda a}da\right| \le \int_0^\infty \rho(a)\omega(a)\overline{\widetilde{R}_r}(a)da = \widetilde{N_r}$$

and

$$\left|\int_0^\infty \rho(a)\omega(a)\bar{R}_s(a)e^{-\lambda a}da\right| \le \int_0^\infty \rho(a)\omega(a)\bar{R}_s(a)da = N_s.$$

Thus, the modulus on the right side of equations (3.17) is less than 1 when $R_1 < 1$ and $R_2 < 1$. However, the left modulus of equations (3.17) is always greater than or equal to 1. By comparing the moduli of both sides of the equation, it is concluded that all solutions have negative real parts. This shows that the infection-free steady state E_0^* of model (3.14) is locally asymptotically stable when $R_1 < 1$ and $R_2 < 1$.

If $R_1 > 1$ or $R_2 > 1$, we define the functions as follows

$$\begin{aligned} f_1(\lambda) &= \frac{\lambda}{c} + 1 - R_1 \frac{\int_0^\infty \rho(a)\omega(a)\overline{\widetilde{R}_r}(a)e^{-\lambda a}da}{\widetilde{N_r}}, \\ f_2(\lambda) &= \frac{\lambda}{c} + 1 - R_2 \frac{\int_0^\infty \rho(a)\omega(a)\bar{R}_s(a)e^{-\lambda a}da}{N_s}. \end{aligned}$$

It is clear that $f_1(0) = 1 - R_1 < 0$ and $f_1(\lambda) \to \infty$ as $\lambda \to \infty$. Similarly, $f_2(0) = 1 - R_2 < 0$ and $f_2(\lambda) \to \infty$ as $\lambda \to \infty$ when $R_2 > 1$. Therefore, there is at least one positive root such that $f_1(\lambda) = 0$ or $f_2(\lambda) = 0$. Thus, the infection-free steady state E_0^* of model (3.14) is unstable when $R_1 > 1$ or $R_2 > 1$.

Theorem 3.2. *The boundary steady state E_1^* of model (3.14) exists if and only if $R_1 > 1$. It is locally asymptotically stable when $R_1 > R_2$ and unstable when $R_2 > R_1$.*

Proof. The boundary steady state E_1^* is brought into the characteristic equation (3.15) to obtain the following characteristic equation

$$\left(\beta_s \bar{T}_1 \int_0^\infty \rho(a)\omega(a)\bar{R}_s(a)e^{-\lambda a}da - c - \lambda\right)\times$$
$$\left[(-d-\lambda)\left(\beta_r \bar{T}_1 \int_0^\infty \rho(a)\omega(a)\overline{\widetilde{R}_r}(a)e^{-\lambda a}da - c - \lambda\right) + \beta_r \bar{V}_{r_1}(c+\lambda)\right] = 0.$$

The eigenvalues are determined by the following equation

$$\frac{\lambda}{c} + 1 = \frac{\beta_s \int_0^\infty \rho(a)\omega(a)\bar{R}_s(a)e^{-\lambda a}da}{\beta_r \widetilde{N_r}}, \tag{3.18}$$

or

$$(d+\lambda)\left(c + \lambda - c\frac{\int_0^\infty \rho(a)\omega(a)\overline{\widetilde{R}_r}(a)e^{-\lambda a}da}{\widetilde{N_r}}\right) + d(R_1 - 1)(c+\lambda) = 0. \tag{3.19}$$

We claim that when $R_2 < R_1$ (i.e. $\beta_s N_s < \beta_r \widetilde{N_r}$), all roots of (3.18) have negative real parts. Otherwise, there exists λ_0 with $\mathrm{Re}(\lambda_0) \geq 0$. This shows that $|\int_0^\infty \rho(a)\omega(a)\bar{R}_s(a)e^{-\lambda_0 a}da| \leq \int_0^\infty \rho(a)\omega(a)\bar{R}_s(a)da = N_s$. Taking modulus of both sides of (3.18) gives

$$\left|\frac{\lambda_0}{c} + 1\right| = \beta_s \frac{|\int_0^\infty \rho(a)\omega(a)\bar{R}_s(a)e^{-\lambda_0 a}da|}{\beta_r \widetilde{N_r}} \leq \frac{\beta_s N_s}{\beta_r \widetilde{N_r}}.$$

This is impossible because the left-hand side is greater than 1 and $\frac{\beta_s N_s}{\beta_r \widetilde{N_r}} < 1$, which leads to a contradiction.

Similarly, all the solutions of the equation (3.19) have negative real parts whenever E_1^* exists, i.e., $R_1 > 1$. Supposing that λ has a non-negative real part, there exists λ_1 with $\mathrm{Re}(\lambda_1) \geq 0$. The modulus of characteristic equation (3.19) can be rewritten as

$$\left|1 + \frac{d(R_1-1)}{d+\lambda_1}\right| = \left|\frac{c\int_0^\infty \rho(a)\omega(a)\overline{\widetilde{R}_r}(a)e^{-\lambda_1 a}da}{(c+\lambda_1)\widetilde{N_r}}\right| \leq 1,$$

which leads to a contradiction. This proves the claim that all roots of characteristic equations have negative real parts when $R_2 < R_1$ and $R_1 > 1$.

When $R_2 > R_1$ (i.e., $\beta_s N_s > \beta_r \widetilde{N_r}$), we let

$$f_3(\lambda) = \frac{\lambda}{c} + 1 - \frac{\beta_s \int_0^\infty \rho(a)\omega(a)\bar{R}_s(a)e^{-\lambda a}da}{\beta_r \widetilde{N_r}}.$$

It is clear that $f_3(0) = 1 - \frac{\beta_s N_s}{\beta_r \widetilde{N_r}} < 0$ and $\lim_{\lambda\to\infty} f_3(\lambda) = \infty$. In this case, there exists a positive root for the equation $f_3(\lambda) = 0$. Thus, the infection-free steady state is unstable when $R_2 > R_1$. On the basis of the above discussion, the boundary steady state E_1^* is locally asymptotically stable when $R_1 > 1$ and $R_2 < R_1$.

Remark. Prior to treatment, the basic reproduction number of the sensitive strain (R_2) must exceed 1; otherwise, the infection would not be established. Furthermore, the basic reproduction number of the resistant strain (R_1) is smaller than that of the sensitive strain due to what is referred to as "mutation-associated fitness loss" — in essence, the mutant virus demonstrates either reduced infection or reproduction capability in the absence of treatment. As a result, the coexistence steady state E_2^* exists before treatment. Although it is challenging to prove the stability of E_2^* under the conditions $R_2 > 1$ and $R_2 > R_1$ before treatment, the existence of both strains is highly probable due to the mutation from the sensitive to the mutant strain. This is also in line with model outcomes that do not take intracellular dynamics into account and aligns with clinical observations (see [27,28] and the references cited therein).

4. Model approximation under therapy

During therapy, the rate of drug-sensitive viral RNA production $\alpha_s(a)$ becomes $(1-\varepsilon_s)\alpha_s(a)$, $\alpha_r(a)$ becomes $(1-\varepsilon_r)\alpha_r(a)$, the degradation rate of virus RNA $\mu(a)$ becomes $\kappa\mu(a)$, the secretion rate of drug-sensitive virus and drug-resistant virus $\rho(a)$ becomes $(1-\eta_s)\rho(a)$ and $(1-\eta_r)\rho(a)$, respectively. The survival probability of an infected cell remains unchanged, i.e. $\omega(a) = e^{-\int_0^a \delta(\tau)d\tau}$, but the survival probability of an infected cell with the infection age a under treatment becomes the following for the two strains

$$\pi_s^t(a) = e^{-\int_0^a [(1-\eta_s)\rho(\tau)+\kappa\mu(\tau)]d\tau}, \quad \pi_r^t(a) = e^{-\int_0^a [(1-\eta_r)\rho(\tau)+\kappa\mu(\tau)]d\tau}.$$

Let R_1^t and R_2^t be the on-treatment reproduction number of the drug-resistant and drug-sensitive strain of model (2.4), respectively. From the calculation in last section, we know

$$R_1^t = \frac{\beta_r s}{dc}\widetilde{N_r^t}, \quad R_2^t = \frac{\beta_s s}{dc}N_s^t,$$

where

$$\widetilde{N_r^t} = \int_0^\infty (1-\eta_r)\rho(a)\left[\pi_r^t(a) + (1-\varepsilon_r)\int_0^a \alpha_r(\tau)\frac{\pi_r^t(a)}{\pi_r^t(\tau)}d\tau\right]\omega(a)da,$$
$$N_s^t = \int_0^\infty (1-\eta_s)\rho(a)\left[\pi_s^t(a) + (1-m)(1-\varepsilon_s)\int_0^a \alpha_s(\tau)\frac{\pi_s^t(a)}{\pi_s^t(\tau)}d\tau\right]\omega(a)da$$

represent the viral burst size of the drug-resistant and drug-sensitive strain, respectively. Using the on-treatment reproduction numbers R_1^t and R_2^t, we have similar results for the model with treatment as in Theorems 3.1 and 3.2.

The above analysis provides asymptotic properties of the model under therapy. In order to study the viral load dynamics during therapy, we assume that the model (2.4) is at the coexistence steady state E_2^* at $t=0$ at the start of treatment (see the remark in last section). We also assume that $\delta(a)$, $\alpha_s(a)$, $\alpha_r(a)$, $\rho(a)$, and $\mu(a)$ are all constants to obtain explicit approximations of the drug-sensitive and resistant viral loads during treatment. In this case, $\omega(a) = e^{-\delta a}$, $\pi(a) = e^{-(\rho+\mu)a}$. It follows from (3.5)-(3.9) that we obtain the solutions of $R_s(a,t)$, $R_r(a,t)$, $\widetilde{R_r}(a,t)$, $I_s(a,t)$, and $I_r(a,t)$ under therapy, given by

$$R_s(a,t) = \begin{cases} \frac{(1-m)A_1}{B_1} + \left(1 - \frac{(1-m)A_1}{B_1}\right)e^{-B_1 a}, & a < t, \\ \frac{(1-m)A_1}{B_1} + \left(\bar{R}_s(a-t) - \frac{(1-m)A_1}{B_1}\right)e^{-B_1 t}, & a \geq t, \end{cases} \tag{4.1}$$

$$R_r(a,t) = \begin{cases} \frac{mA_1}{B_2}(1-e^{-B_2 a}), & a < t, \\ \frac{mA_1}{B_2} + \left(\bar{R}_r(a-t) - \frac{mA_1}{B_2}\right)e^{-B_2 t}, & a \geq t, \end{cases} \tag{4.2}$$

$$\widetilde{R_r}(a,t) = \begin{cases} \frac{A_2}{B_2} + (1-\frac{A_2}{B_2})e^{-B_2 a}, & a < t, \\ \frac{A_2}{B_2} + \left(\widetilde{\bar{R}_r}(a-t) - \frac{A_2}{B_2}\right)e^{-B_2 t}, & a \geq t, \end{cases} \tag{4.3}$$

$$I_s(a,t) = \begin{cases} \beta_s V_s(t-a)T(t-a)e^{-\delta a}, & a < t, \\ \bar{I}_s(a-t)e^{-\delta t}, & a \geq t, \end{cases} \tag{4.4}$$

and

$$I_r(a,t) = \begin{cases} \beta_r V_r(t-a)T(t-a)e^{-\delta a}, & a < t, \\ \bar{I}_r(a-t)e^{-\delta t}, & a \geq t, \end{cases} \tag{4.5}$$

where $A_1 = (1-\varepsilon_s)\alpha_s$, $B_1 = (1-\eta_s)\rho + k\mu$, $A_2 = (1-\varepsilon_r)\alpha_r$, and $B_2 = (1-\eta_r)\rho + k\mu$. $\bar{R}_s(a)$, $\bar{R}_r(a)$, $\widetilde{\bar{R}_r}(a)$, $\bar{I}_s(a)$, and $\bar{I}_r(a)$ are the pre-treatment steady state distributions of intracellular viral RNA and infected cells with drug-sensitive and drug-resistant virus, respectively. From (3.1) and (3.2), we obtain these steady states

$$\begin{aligned} &\bar{I}_s(a) = \beta_s \bar{V}_s \bar{T} e^{-\delta a}, \ \bar{I}_r(a) = \beta_r \bar{V}_r \bar{T} e^{-\delta a}, \ \bar{R}_s(a) = (1-m)\frac{\alpha_s}{\rho+\mu} + \left(1 - (1-m)\frac{\alpha_s}{\rho+\mu}\right)e^{-(\rho+\mu)a}, \\ &\bar{R}_r(a) = m\frac{\alpha_s}{\rho+\mu}(1-e^{-(\rho+\mu)a}), \ \widetilde{\bar{R}_r}(a) = \frac{\alpha_r}{\rho+\mu} + \left(1 - \frac{\alpha_r}{\rho+\mu}\right)e^{-(\rho+\mu)a}. \end{aligned} \tag{4.6}$$

It should be noted that for $a > t$, $I_s(a,t) = \bar{I}_s(a-t)e^{-\delta t} = \beta_s \bar{V}_s \bar{T} e^{-\delta a}$, $I_r(a,t) = \bar{I}_r(a-t)e^{-\delta t} = \beta_r \bar{V}_r \bar{T} e^{-\delta a}$. Therefore, cells infected before the therapy was administered, i.e., for $a > t$, maintain their steady state age distribution even after therapy starts.

We first approximate the viral load during therapy by assuming that the infected cells of the two strains keep their stable state distribution before treatment, which implies that $I_s(a,t) = \bar{I}_s(a) = \beta_s \bar{V}_s \bar{T} e^{-\delta a}$, $I_r(a,t) = \bar{I}_r(a) = \beta_r \bar{V}_r \bar{T} e^{-\delta a}$. This is equivalent to assuming that the new infection (i.e. $a < t$) occurs at rate $\beta_s \bar{V}_s \bar{T}$ and $\beta_r \bar{V}_r \bar{T}$ instead of $\beta_s V_s(t-a)T(t-a)$ and $\beta_r V_r(t-a)T(t-a)$ after treatment starts. This assumption is reasonable only in a short period of time after the start of treatment, because the new infection rate will decrease in the presence of effective treatment. According to this assumption, $V_s(t)$ and $V_r(t)$ of (2.4) can be written as

$$\begin{aligned} \frac{dV_s(t)}{dt} &= (1-\eta_s)\int_0^\infty \rho R_s(a,t)\bar{I}_s(a)da - cV_s(t), \\ \frac{dV_r(t)}{dt} &= (1-\eta_r)\int_0^\infty \rho R_r(a,t)\bar{I}_s(a)da + (1-\eta_r)\int_0^\infty \rho \widetilde{R_r}(a,t)\bar{I}_r(a)da - cV_r(t). \end{aligned} \tag{4.7}$$

It follows from (4.1) that we divide the integral of the first equation into two parts as follows

$$\int_0^\infty R_s(a,t)\bar{I}_s(a)da = \int_0^t R_s(a,t)\bar{I}_s(a)da + \int_t^\infty R_s(a,t)\bar{I}_s(a)da.$$

Next, we calculate two integrals separately, given by

$$\int_0^t R_s(a,t)\bar{I}_s(a)da = \beta_s\bar{V}_s\bar{T}\left[\frac{(1-m)A_1+\delta}{\delta(B_1+\delta)} - \frac{(1-m)A_1}{\delta B_1}e^{-\delta t} + \frac{(1-m)A_1-B_1}{B_1(B_1+\delta)}e^{-(B_1+\delta)t}\right],$$

$$\int_t^\infty R_s(a,t)\bar{I}_s(a)da = \beta_s\bar{V}_s\bar{T}\left[\frac{(1-m)A_1}{\delta B_1}e^{-\delta t} + \left(\frac{N_s}{\rho} - \frac{(1-m)A_1}{B_1\delta}\right)e^{-(B_1+\delta)t}\right],$$

where $N_s = \int_0^\infty \rho\bar{R}_s(a)\omega(a)da = \rho\frac{\delta+(1-m)\alpha_s}{\delta(\rho+\mu+\delta)}$. We add the above two integrals and obtain

$$\int_0^\infty R_s(a,t)\bar{I}_s(a)da = \frac{c}{N_s}\bar{V}_s\left[\frac{(1-m)A_1+\delta}{\delta(B_1+\delta)} + \left(\frac{N_s}{\rho} - \frac{(1-m)A_1+\delta}{\delta(B_1+\delta)}\right)e^{-(B_1+\delta)t}\right]. \tag{4.8}$$

Taking (4.8) into the first equation of (4.7), we have

$$\frac{dV_s(t)}{dt} = (1-\eta_s)\frac{\rho c}{N_s}\bar{V}_s\left[\frac{(1-m)A_1+\delta}{\delta(B_1+\delta)} + \left(\frac{N_s}{\rho} - \frac{(1-m)A_1+\delta}{\delta(B_1+\delta)}\right)e^{-(B_1+\delta)t}\right] - cV_s(t).$$

The solution of $V_s(t)$ is obtained by the constant variation method

$$\begin{aligned}\frac{V_s(t)}{V_{s0}} = {} & e^{-ct} + (1-\eta_s)\frac{c\rho}{N_s}\left[\frac{(1-m)A_1+\delta}{c\delta(B_1+\delta)}(1-e^{-ct})\right.\\ & \left.+\frac{1}{B_1+\delta-c}\left(\frac{N_s}{\rho} - \frac{(1-m)A_1+\delta}{\delta(B_1+\delta)}\right)(e^{-ct}-e^{-(B_1+\delta)t})\right],\end{aligned} \tag{4.9}$$

where $V_{s0} = \bar{V}_s$ is the baseline with drug sensitive viral load before treatment begins. The rate of the new infection is assumed to be $\beta_s\bar{V}_s\bar{T}$ within a short period of time after the start of treatment. We call (4.9) the *short-term* approximation of drug sensitive viral decline during treatment.

Alternatively, we can approximate the viral load change by ignoring all new infections after treatment starts. As a result of (4.4), $I_s(a,t) = 0$ for $a < t$, and $I_s(a,t) = \bar{I}_s(a-t)e^{-\delta t} = \beta_s\bar{V}_s\bar{T}e^{-\delta a}$ for $a \geq t$. Therefore, the equation of $V_s(t)$ in (4.7) can be rewritten as

$$\frac{dV_s(t)}{dt} = (1-\eta_s)\int_t^\infty \rho R_s(a,t)I_s(a,t)da - cV_s(t).$$

Calculating the integral, we have

$$\frac{dV_s(t)}{dt} = (1-\eta_s)\frac{\rho c}{N_s}\bar{V}_s\left[\frac{(1-m)A_1}{\delta B_1}e^{-\delta t} + \left(\frac{N_s}{\rho} - \frac{(1-m)A_1}{B_1\delta}\right)e^{-(B_1+\delta)t}\right] - cV_s(t).$$

Solving for $V_s(t)$, we obtain

$$\begin{aligned}\frac{V_s(t)}{V_{s0}} = {} & e^{-ct} + (1-\eta_s)\frac{c\rho}{N_s}\left[\frac{(1-m)A_1}{B_1\delta(\delta-c)}(e^{-ct}-e^{-\delta t})\right.\\ & \left.+\frac{1}{B_1+\delta-c}\left(\frac{N_s}{\rho} - \frac{(1-m)A_1}{B_1\delta}\right)(e^{-ct}-e^{-(B_1+\delta)t})\right].\end{aligned} \tag{4.10}$$

Under this approximation, we ignore all new infections during treatment (i.e. when $a < t$, $I_s(a,t) = 0$). This assumption is reasonable, particularly after a long-term effective therapy, which can greatly suppress the production of drug-sensitive viruses. We call (4.10) a *long-term* approximation of the decrease of drug-sensitive viruses after treatment.

In the following, we perform similar approximations for the resistant strain. We start with the short-term approximation. We get the following integrals from (4.2) and (4.3)

$$\int_0^\infty R_r(a,t)\bar{I}_s(a)da = \int_0^t R_r(a,t)\bar{I}_s(a)da + \int_t^\infty R_r(a,t)\bar{I}_s(a)da,$$

$$\int_0^\infty \widetilde{R}_r(a,t)\bar{I}_r(a)da = \int_0^t \widetilde{R}_r(a,t)\bar{I}_r(a)da + \int_t^\infty \widetilde{R}_r(a,t)\bar{I}_r(a)da.$$

We calculate the integrals

$$\int_0^t R_r(a,t)\bar{I}_s(a)da = \frac{mA_1}{B_2}\beta_s\bar{V}_s\bar{T}\left(\frac{B_2}{\delta(B_2+\delta)} - \frac{1}{\delta}e^{-\delta t} + \frac{1}{B_2+\delta}e^{-(B_2+\delta)t}\right),$$

$$\int_t^\infty R_r(a,t)\bar{I}_s(a)da = \beta_s\bar{V}_s\bar{T}\left[\frac{mA_1}{\delta B_2}e^{-\delta t} + \left(\frac{N_r}{\rho} - \frac{mA_1}{B_2\delta}\right)e^{-(B_2+\delta)t}\right],$$

$$\int_0^t \widetilde{R_r}(a,t)\bar{I}_r(a)da = \beta_r\bar{V}_r\bar{T}\left(\frac{A_2+\delta}{\delta(B_2+\delta)} - \frac{A_2}{B_2\delta}e^{-\delta t} + \frac{A_2-B_2}{B_2(B_2+\delta)}e^{-(B_2+\delta)t}\right),$$

and

$$\int_t^\infty \widetilde{R_r}(a,t)\bar{I}_r(a)da = \beta_r\bar{V}_r\bar{T}\left[\frac{A_2}{\delta B_2}e^{-\delta t} + \left(\frac{\widetilde{N_r}}{\rho} - \frac{A_2}{B_2\delta}\right)e^{-(B_2+\delta)t}\right],$$

where $N_r = \int_0^\infty \rho\bar{R}_r(a)\omega(a)da = \rho\frac{m\alpha_s}{\delta(\rho+\mu+\delta)}$, $\widetilde{N_r} = \int_0^\infty \rho\overline{\widetilde{R}_r}(a)\omega(a)da = \rho\frac{\alpha_r+\delta}{\delta(\rho+\mu+\delta)}$. We add the above integrals and obtain

$$\begin{aligned}
&\int_0^\infty R_r(a,t)\bar{I}_s(a)da = \frac{c\bar{V}_s}{N_s}\left[\frac{mA_1}{\delta(B_2+\delta)} + \left(\frac{N_r}{\rho} - \frac{mA_1}{\delta(B_2+\delta)}\right)e^{-(B_2+\delta)t}\right],\\
&\int_0^\infty \widetilde{R_r}(a,t)\bar{I}_r(a)da = \frac{c\beta_r\bar{V}_r}{\beta_s N_s}\left[\frac{A_2+\delta}{\delta(B_2+\delta)} + \left(\frac{\widetilde{N_r}}{\rho} - \frac{A_2+\delta}{\delta(B_2+\delta)}\right)e^{-(B_2+\delta)t}\right].
\end{aligned} \tag{4.11}$$

Plugging (4.11) into $V_r(t)$ of (4.7), we have

$$\begin{aligned}
\frac{\mathrm{d}V_r(t)}{\mathrm{d}t} =&(1-\eta_r)\rho\frac{c\bar{V}_s}{N_s}\left[\frac{mA_1}{\delta(B_2+\delta)} + \left(\frac{N_r}{\rho} - \frac{mA_1}{\delta(B_2+\delta)}\right)e^{-(B_2+\delta)t}\right]\\
&+(1-\eta_r)\rho\frac{c\beta_r\bar{V}_r}{\beta_s N_s}\left[\frac{A_2+\delta}{\delta(B_2+\delta)} + \left(\frac{\widetilde{N_r}}{\rho} - \frac{A_2+\delta}{\delta(B_2+\delta)}\right)e^{-(B_2+\delta)t}\right] - cV_r(t),
\end{aligned}$$

and the solution of $V_r(t)$ is obtained by the constant variation method

$$\begin{aligned}
\frac{V_r(t)}{V_{r0}} =&e^{-ct} + (1-\eta_r)\frac{c\rho}{N_s}\frac{V_{s0}}{V_{r0}}\left[\frac{mA_1}{c\delta(B_2+\delta)}(1-e^{-ct})\right.\\
&\left.+\frac{1}{B_2+\delta-c}\left(\frac{N_r}{\rho} - \frac{mA_1}{\delta(B_2+\delta)}\right)(e^{-ct} - e^{-(B_2+\delta)t})\right]\\
&+(1-\eta_r)\frac{c\beta_r\rho}{\beta_s N_s}\left[\frac{A_2+\delta}{c\delta(B_2+\delta)}(1-e^{-ct})\right.\\
&\left.+\frac{1}{B_2+\delta-c}\left(\frac{\widetilde{N_r}}{\rho} - \frac{A_2+\delta}{\delta(B_2+\delta)}\right)(e^{-ct} - e^{-(B_2+\delta)t})\right],
\end{aligned} \tag{4.12}$$

where $V_{s0} = \bar{V}_s$, $V_{r0} = \bar{V}_r$ are the baseline with drug-sensitive and drug-resistant viral load before treatment begins, respectively. The rate of new infection is assumed to be $\beta_r\bar{V}_r\bar{T}$ and $\beta_s\bar{V}_s\bar{T}$ within a short period of time after the start of treatment. We call (4.12) the *short-term* approximation of drug resistance viral decline during treatment.

Similarly, we will obtain the long-term approximation of the resistant viral load. We ignore all new infections after treatment starts. From (4.5), we have $I_r(a,t) = 0$, $I_s(a,t) = 0$ for $a < t$, and $I_r(a,t) = \bar{I}_r(a-t)e^{-\delta t} = \beta_r\bar{V}_r\bar{T}e^{-\delta a}$, $I_s(a,t) = \bar{I}_s(a-t)e^{-\delta t} = \beta_s\bar{V}_s\bar{T}e^{-\delta a}$ for $a \geq t$.

The $V_r(t)$ equation for model (2.4) is rewritten as

$$\begin{aligned}
\frac{dV_r(t)}{dt} &= (1-\eta_r)\int_t^\infty \rho R_r(a,t)I_s(a,t)da + (1-\eta_r)\int_t^\infty \rho\widetilde{R_r}(a,t)I_r(a,t)da - cV_r(t)\\
&= (1-\eta_r)\frac{\bar{V}_s c\rho}{N_s}\left[\frac{mA_1}{B_2\delta}e^{-\delta t} + \left(\frac{N_r}{\rho} - \frac{mA_1}{\delta B_2}\right)e^{-(B_2+\delta)t}\right]\\
&\quad+(1-\eta_r)\frac{\beta_r\bar{V}_r c\rho}{\beta_s N_s}\left[\frac{A_2}{B_2\delta}e^{-\delta t} + \left(\frac{\widetilde{N_r}}{\rho} - \frac{A_2}{B_2\delta}\right)e^{-(B_2+\delta)t}\right] - cV_r(t).
\end{aligned}$$

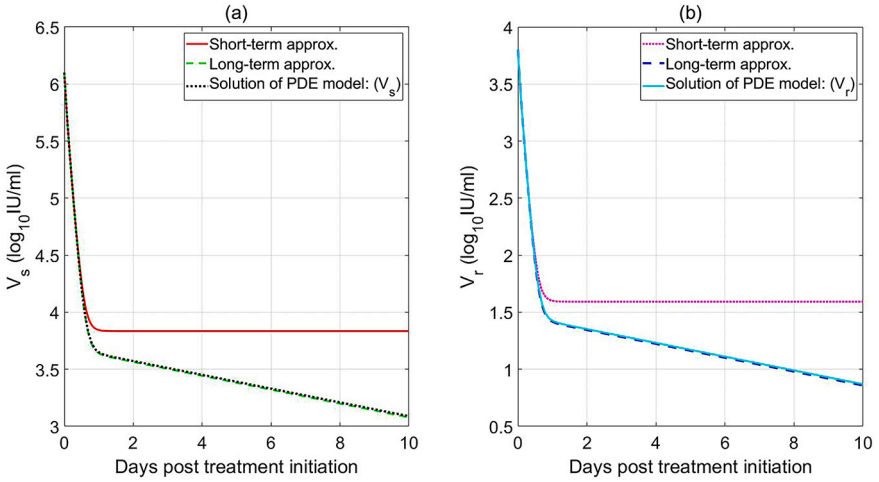

Fig. 3. Comparison of the multiscale model with their approximate solutions. Panels (a) and (b) show the graphs of drug-sensitive and drug-resistant viruses under drug treatment, respectively. The black dotted line and the blue-green solid line represent the numerical solutions of V_s and V_r from the PDE model. The red dotted line and red purple solid line represent short-term approximations for the two strains. The green dotted line and blue dotted line represent long-term approximations for the two strains. The values of the model parameters are shown in Table 1.

Solving for $V_r(t)$, we obtain

$$\begin{aligned}\frac{V_r(t)}{V_{r0}} =& e^{-ct} + (1-\eta_r)\frac{c\rho V_{s0}}{N_s V_{r0}}\left[\frac{mA_1}{B_2\delta(\delta-c)}(e^{-ct}-e^{-\delta t})\right.\\ &\left.+\frac{1}{B_2+\delta-c}\left(\frac{N_r}{\rho}-\frac{mA_1}{\delta B_2}\right)(e^{-ct}-e^{-(B_2+\delta)t})\right]\\ &+(1-\eta_r)\frac{\beta_r c\rho}{\beta_s N_s}\left[\frac{A_2}{B_2\delta(\delta-c)}(e^{-ct}-e^{-\delta t})\right.\\ &\left.+\frac{1}{B_2+\delta-c}\left(\frac{\widetilde{N_r}}{\rho}-\frac{A_2}{B_2\delta}\right)(e^{-ct}-e^{-(B_2+\delta)t})\right].\end{aligned} \tag{4.13}$$

The formula (4.13) is referred to as the *long-term* approximation for the decrease of drug-resistant viruses during treatment.

We compare the solution of the multiscale PDE model (2.4) with approximations for drug-sensitive and drug-resistant virus strains using numerical simulation. Fig. 3 shows that the short-term approximations for drug-sensitive (4.9) (red dotted line in Fig. 3(a)) and drug-resistant (4.12) (purple solid line in Fig. 3(b)) virus strains are consistent with the PDE model solution (2.4) (black dotted line in Fig. 3(a) and blue-green solid line in Fig. 3(b)) in the early stage of treatment. However, the short-term approximations quickly approach the steady state, which is higher than the PDE model solution (2.4). The long-term approximations for drug-sensitive (4.10) (green dotted line in Fig. 3(a)) and drug-resistant (4.13) (blue dotted line in Fig. 3(b)) virus strains provide good approximations to the PDE model solution (2.4) (Fig. 3).

5. Effect of drug therapy on multiscale model dynamics

The last section shows that the long-term approximate equations (4.10) and (4.13) for the two strains are in agreement with the solution of the multiscale PDE model (2.4). In this section, we use the long-term approximation to study the influence of DAAs on the viral load change of drug-sensitive and drug-resistant viruses during treatment.

To investigate the change of drug-sensitive viral load during treatment, we reorganize the long-term approximation (4.10) as follows:

$$\frac{V_s(t)}{V_{s0}} = C_1 e^{-ct} + C_2 e^{-(B_1+\delta)t} + C_3 e^{-\delta t},$$

where

$$\begin{aligned}C_1 =& 1-(1-\eta_s)\frac{c\rho}{N_s}\left[\frac{(1-m)A_1}{B_1\delta(c-\delta)}+\frac{1}{c-\delta-B_1}\left(\frac{N_s}{\rho}-\frac{(1-m)A_1}{B_1\delta}\right)\right],\\ C_2 =& (1-\eta_s)\frac{c\rho}{N_s}\frac{1}{c-\delta-B_1}\left(\frac{N_s}{\rho}-\frac{(1-m)A_1}{B_1\delta}\right),\\ C_3 =& (1-\eta_s)\frac{c\rho}{N_s}\frac{(1-m)A_1}{B_1\delta(c-\delta)}.\end{aligned}$$

Table 1
Parameter values in numerical simulation.

Parameter	Description	Values	References
s	Recruitment rate of uninfected cells	1.30×10^{5} cells mL^{-1} day^{-1}	[16]
d	Death rate of uninfected cells	0.01 day^{-1}	[16]
β_s	Infection rate of target cells by drug-sensitive virus	5×10^{-8} mL day^{-1}virions^{-1}	[29]
β_r	Infection rate of target cells by drug-resistant virus	4.99×10^{-8} mL day^{-1}virions^{-1}	[29]
δ	Death rate of infected cells	0.14 day^{-1}	[29]
ρ	Assembly/secretion rate of viral RNA	8.18 day^{-1}	[29]
κ	Drug effect of enhancing RNA degradation	4.94	[29]
μ	Degradation rate of viral RNA	1 day^{-1}	[29]
c	Clearance rate of free virus	22.3 day^{-1}	[16]
m	Mutation rate from sensitive strain to resistant strain	10^{-5} per copied nucleotide	[30]
ε_s	Drug effect of inhibiting drug-sensitive viral RNA production	0.992	[29]
ε_r	Drug effect of inhibiting drug-resistant viral RNA production	0.99	[30]
η_s	Drug effect of blocking assembly/ secretion of drug-sensitive viral RNA	0.56	[29]
η_r	Drug effect of blocking assembly/ secretion of drug-resistant viral RNA	0.55	[30]
α_s	Production rate of intracellular drug-sensitive viral RNA	40 virions cell^{-1}	[29]
α_r	Production rate of intracellular drug-resistant viral RNA	38 virions cell^{-1}	[30]

The approximation contains three exponential terms, namely e^{-ct}, $e^{-(B_1+\delta)t}$, and $e^{-\delta t}$, where $B_1=(1-\eta_s)\rho+k\mu$. The first term represents the elimination of drug-sensitive viruses, the second term represents the export and degradation of intracellular drug-sensitive virus RNA, and the elimination of infected cells, while the third term represents the death of infected cells. After the start of treatment, the decrease in the three viral loads depends not only on the exponents but also on the coefficients before the exponential terms.

When plotting the viral load change on the logarithmic scale with base 10, the duration of the virus decline in the first stage is denoted as D_1. It is the time when the two curves $\log_{10}(C_1e^{-ct})$ and $\log_{10}(C_2e^{-(B_1+\delta)t})$ intersect, and is given as follows:

$$D_1=\frac{\ln(\frac{C_1}{C_2})}{c-(B_1+\delta)}.$$

Similarly, we obtain the duration of virus decline in the second stage, which is defined as D_2:

$$D_2=\frac{\ln(\frac{C_2}{C_3})}{B_1}.$$

If η_s tends to 1, then $C_1\gg C_2$, and the drug-sensitive virus decreases significantly at the rate of slope proportional to c (i.e. $-\log_{10}e\times c$) in the first stage. If ε_s tends to 1, then $A_1=(1-\varepsilon_s)\alpha_s$ approaches 0. Hence, we obtain $C_2\gg C_3$, and drug-sensitive virus showed an obvious decreasing trend with slope proportional to $B_1+\delta$ (i.e. $-\log_{10}e\times(B_1+\delta)$). We can confirm these theoretical analyses in Fig. 4. From the figure, we can conclude that hindering the assembly and secretion of drug-sensitive virus in plasma ($\eta_s=0.99$) and inhibiting the production of intracellular drug-sensitive virus RNA ($\varepsilon_s=0.99$) lead to a significant decrease in drug-sensitive virus load in three stages, with slopes proportional to c, $(1-\eta_s)\rho+k\mu+\delta$, and δ, respectively (blue solid line).

When ε_s decreases, the drug-sensitive virus decreases continuously with slope proportional to c in the first stage and disappears in the second stage with slope proportional to $(1-\eta_s)\rho+k\mu+\delta$ (green dotted line and blue-green dotted line). When $\eta_s=0.01$, the decline with slope proportional to c of drug-sensitive virus in the first stage is invisible (red dashed). These results can explain why the estimated value of viral clearance rate c is significantly higher in DAA-based treatment for HCV compared to traditional interferon-based treatment, as reported in [17].

Next, we study the effect of drug treatment on the decrease of drug-resistant viral load. Similarly, equation (4.13) can be rewritten as

$$\frac{V_r(t)}{V_{r0}}=C_4e^{-ct}+C_5e^{-(B_2+\delta)t}+C_6e^{-\delta t},$$

where

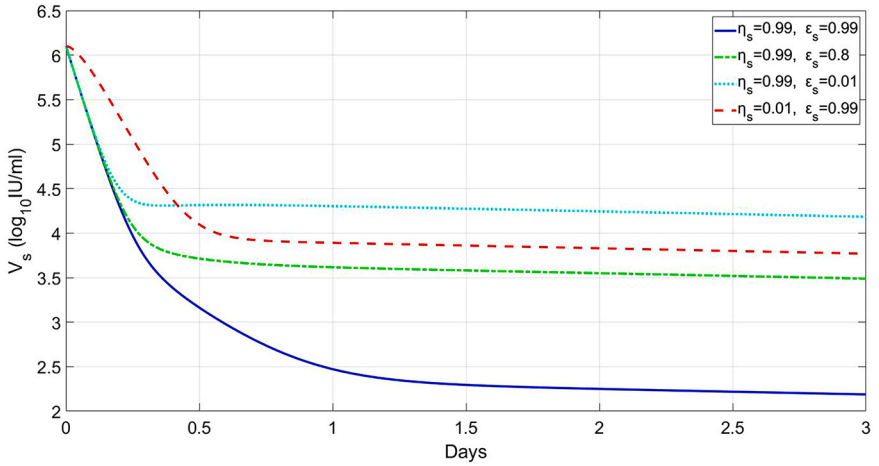

Fig. 4. Effect of treatment on the change of drug-sensitive viral load. The long-term approximation of drug-sensitive viral load simulates different combinations of drug efficacies η_s and ε_s. Other parameter values are the same in Table 1.

$$C_4 = 1-(1-\eta_r)\frac{c\rho}{N_s}\left[\frac{V_{s0}}{V_{r0}}\left(\frac{mA_1}{B_2\delta(c-\delta)}+\frac{1}{c-B_2-\delta}\left(\frac{N_r}{\rho}-\frac{mA_1}{\delta B_2}\right)\right)\right.$$
$$\left.+\frac{\beta_r}{\beta_s}\left(\frac{A_2}{B_2\delta(c-\delta)}+\frac{1}{c-B_2-\delta}\left(\frac{\widetilde{N_r}}{\rho}-\frac{A_2}{B_2\delta}\right)\right)\right],$$
$$C_5 = (1-\eta_r)\frac{c\rho}{N_s(c-B_2-\delta)}\left[\frac{V_{s0}}{V_{r0}}\left(\frac{N_r}{\rho}-\frac{mA_1}{\delta B_2}\right)+\frac{\beta_r}{\beta_s}\left(\frac{\widetilde{N_r}}{\rho}-\frac{A_2}{B_2\delta}\right)\right],$$
$$C_6 = (1-\eta_r)\frac{c\rho}{N_s B_2\delta(c-\delta)}\left(\frac{V_{s0}}{V_{r0}}mA_1+\frac{\beta_r A_2}{\beta_s}\right),$$

where $B_2=(1-\eta_r)\rho+k\mu$, $A_2=(1-\varepsilon_r)\alpha_r$, and $A_1=(1-\varepsilon_s)\alpha_s$. There are also three exponential terms in this approximation, and the explanation is similar to the above so it is not repeated here. Different from the expression of drug-sensitive viral load, the coefficients of drug-resistant viral load are not only related to ε_r, but also to ε_s.

The duration of the first and second stages of decline for drug-resistant viruses are denoted by D_3 and D_4, respectively, and are calculated as follows:

$$D_3=\frac{\ln\left(\frac{C_4}{C_5}\right)}{c-(B_2+\delta)},\quad D_4=\frac{\ln\left(\frac{C_5}{C_6}\right)}{B_2}.$$

When η_r tends to 1, the drug-resistant virus load decreases significantly in the first stage with a slope proportional to c, as $C_4 \gg C_5$. If ε_s and ε_r tend to 1, $A_1=(1-\varepsilon_s)\alpha_s$ and $A_2=(1-\varepsilon_r)\alpha_r$ are very small. In this case, $C_5 \gg C_6$ and the drug-resistant virus shows a decrease with a slope proportional to $B_2+\delta$. Numerical simulations (Fig. 5) confirm these theoretical analyses. When the treatment blocks the assembly/secretion of drug-resistant virus in plasma ($\eta_r=0.99$) and inhibits the RNA production of both viruses in cells ($\varepsilon_s=0.99,\ \varepsilon_r=0.99$), the viral load of drug-resistant virus decreases in three stages (blue dotted line), with slopes proportional to c, $(1-\eta_r)\rho+k\mu+\delta$, and δ. If $\eta_r=0.01$, the first-stage decline of drug-resistant virus with slope proportional to c becomes invisible (blue-green dotted line).

Fig. 5 shows that the green dot-dotted line coincides with the blue dotted line, and ε_r is different, but inhibiting the production of intracellular drug-resistant virus RNA still has a curative effect. This suggests that the curative effect of η_r is more effective than that of ε_r in this case. The comparison between the blue-green dotted line and the red-purple solid line illustrates this phenomenon. Moreover, when these two drug efficacies are the same, the influence of η_r is stronger on viral load reduction. The comparison between the blue-green dotted line and the red dotted line shows that the drug efficacy ε_s has little effect on the reduction of drug-resistant virus load, while the comparison between the blue-green dotted line and the red-purple solid line shows that ε_r has a greater effect than ε_s. In general, these three drug efficacies can have different effects on the reduction of drug-resistant virus load.

6. Conclusion and discussion

In studying the effect of DAAs in treating patients, treatment analysis is facilitated by considering multiscale models of intracellular viral dynamics, as these drugs directly interfere with specific steps of the HCV life cycle. Specific targeted antiviral therapy for HCV is considered an attractive strategy, with the goal of achieving lower viral load, shorter treatment duration, and better drug resistance. Due to the high replication rate of HCV and the fallibility of viral RNA polymerase, a large number of viral mutations are produced, making the emergence of drug-resistant variants a major obstacle to such treatment. During treatment, variants that are resistant to the specific drugs used are selected, and these drug-resistant viruses have an adaptive advantage over sensitive viruses

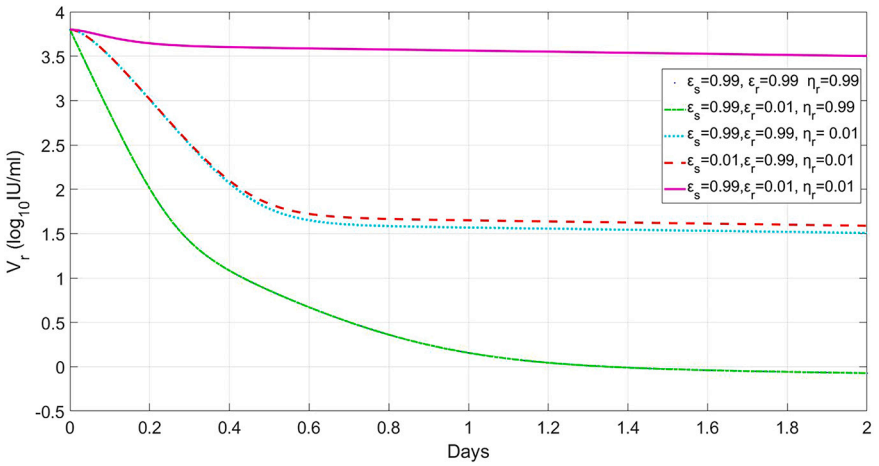

Fig. 5. Effect of treatment on the change of drug-resistant viral load. The long-term approximation of drug-resistant virus load simulates different combinations of drug efficacies ε_s, ε_r, and η_r. Other parameter values are the same in Table 1.

under drug pressure, allowing them to rapidly evolve and dominate the virus population, particularly during monotherapy. To study the dynamic behavior of HCV before and after treatment, this paper proposes a multiscale model that includes the age structure of infection and two strains of viruses.

We have calculated three steady states of the model prior to treatment and analyzed the conditions for the existence of steady states and their stability. Specifically, we have found that when the basic reproductive numbers R_1 and R_2 are both less than 1, the infection-free steady-state is locally asymptotically stable. Here, R_1 and R_2 represent the basic reproductive numbers of the resistant and sensitive strains, respectively. Moreover, we have found that the boundary steady state exists if and only if R_1 is greater than 1, which means that only the steady state of drug-resistant virus exists. Additionally, we have shown that if R_1 is greater than R_2 and R_1 is greater than 1, the boundary steady state is locally asymptotically stable.

Furthermore, we have obtained approximations of the solutions of the multiscale model under certain assumptions. Specifically, we have used the approximate assumption that there is no new infection during treatment, which is referred to as the long-term approximation, and found that it is consistent with the solution of the multiscale model. Using these two long-term approximations, we have studied the effect of drug treatment on the dynamics of the two strains.

Multiscale models provide a clear explanation of the potential effects of DAAs on the production and degradation of intracellular sensitive and resistant viral RNA, as well as on the assembly and secretion of viruses to the circulation. The results indicate that if treatment can effectively block viral secretion, then the initial reduction in viral load reflects the clearance of viruses in plasma. If intracellular RNA production is also significantly inhibited during treatment, a visible second-phase viral decline will occur, reflecting the loss rate of the HCV replication complex and the mortality rate of infected cells. The third phase reflects the mortality rate of infected cells. To treat drug-resistant viruses, more optimal drug combinations can be identified, such as enhancing the drug effect that blocks the secretion of drug-resistant viruses, as its antiviral effect is superior to that of the other two efficacies, which helps reduce the viral load of drug-resistant viruses and achieve the desired treatment outcome.

Declaration of competing interest

None of the authors have any financial or non-financial interests that are directly or indirectly related to this work.

Data availability

No data was used for the research described in the article.

Acknowledgements

X. Wang was supported by the National Natural Science Foundation of China (No. 12171413), the Natural Science Foundation of Henan Province (222300420016), and the Program for Innovative Research Team in Science and Technology in Universities of Henan Province (21IRTSTHN014). L. Rong was supported by the NSF grants DMS-1950254 and DMS-2324692.

References

[1] S. Lanini, P.J. Easterbrook, A. Zumla, et al., Hepatitis C: global epidemiology and strategies for control, Clin. Microbiol. Infect. 22 (10) (2016) 833–838, https://doi.org/10.1016/j.cmi.2016.07.035.
[2] World Health Organization, Hepatitis C, https://www.who.int/news-room/fact-sheets/detail/hepatitis-c, 2023. (Accessed 12 July 2023).
[3] G.R. Foster, Past, present, and future hepatitis C treatments, Seminars in Liver Disease 24 (2004) 97–104, https://doi.org/10.1055/s-2004-832934.

[4] D.N. Fusco, R.T. Chung, Novel therapies for hepatitis C: insights from the structure of the virus, Annu. Rev. Med. 63 (1) (2012) 373–387, https://doi.org/10.1146/annurev-med-042010-085715.
[5] Y. Koizumi, H. Ohashi, S. Nakajima, et al., Quantifying antiviral activity optimizes drug combinations against hepatitis C virus infection, Proc. Natl. Acad. Sci. 114 (8) (2017) 1922–1927, https://doi.org/10.1073/pnas.1610197114.
[6] E. Herrmann, A.U. Neumann, J.M. Schmidt, et al., Hepatitis C virus kinetics, Antivir. Ther. 5 (2) (2000) 85–90, https://doi.org/10.1097/00042737-200604000-00006.
[7] J. Guedj, L. Rong, H. Dahari, A.S. Perelson, A perspective on modelling hepatitis C virus infection, J. Viral Hepatitis 17 (12) (2010) 825–833, https://doi.org/10.1111/j.1365-2893.2010.01348.x.
[8] L. Rong, A.S. Perelson, Treatment of hepatitis C virus infection with interferon and small molecule direct antivirals: viral kinetics and modeling, Critical Reviews in Immunology 30 (2) (2010) 131–148, https://doi.org/10.1615/CritRevImmunol.v30.i2.30.
[9] M.N. Jan, G. Zaman, et al., Optimal control application to the epidemiology of HBV and HCV co-infection, Int. J. Biomath. 15 (03) (2022) 2150101, https://doi.org/10.1142/S1793524521501011.
[10] J. Guedj, A.U. Neumann, Understanding hepatitis C viral dynamics with direct-acting antiviral agents due to the interplay between intracellular replication and cellular infection dynamics, J. Theor. Biol. 267 (3) (2010) 330–340, https://doi.org/10.1016/j.jtbi.2010.08.036.
[11] L. Rong, A.S. Perelson, Mathematical analysis of multiscale models for hepatitis C virus dynamics under therapy with direct-acting antiviral agents, Math. Biosci. 245 (2013) 22–30, https://doi.org/10.1016/j.mbs.2013.04.012.
[12] L. Rong, J. Guedj, H. Dahari, et al., Analysis of hepatitis C virus decline during treatment with the protease inhibitor danoprevir using a multiscale model, PLoS Comput. Biol. 9 (3) (2013) e1002959, https://doi.org/10.1371/journal.pcbi.1002959.
[13] P.W. Nelson, M.A. Gilchrist, D. Coombs, et al., An age-structured model of HIV infection that allows for variations in the production rate of viral particles and the death rate of productively infected cells, Math. Biosci. Eng. 1 (2) (2017) 267–288, https://doi.org/10.3934/mbe.2004.1.267.
[14] B.M. Quintela, J.M. Conway, J.M. Hyman, et al., A new age-structured multiscale model of the hepatitis C virus life-cycle during infection and therapy with direct-acting antiviral agents, Front. Microbiol. 9 (2018) 601, https://doi.org/10.3389/fmicb.2018.00601.
[15] V. Reinharz, H. Dahari, D. Barash, Numerical schemes for solving and optimizing multiscale models with age of hepatitis C virus dynamics, Math. Biosci. 300 (2018) 1–13, https://doi.org/10.1016/j.mbs.2018.03.011.
[16] K. Kitagawa, S. Nakaoka, Y. Asai, et al., A PDE multiscale model of hepatitis C virus infection can be transformed to a model of ODEs, J. Theor. Biol. 448 (2018) 80–85, https://doi.org/10.1016/j.jtbi.2018.04.006.
[17] J. Guedj, H. Dahari, L.B. Rong, et al., Modeling shows that the NS5A inhibitor daclatasvir has two modes of action and yields a shorter estimate of the hepatitis C virus half-life, Proc. Natl. Acad. Sci. 110 (10) (2013) 3991–3996, https://doi.org/10.1073/pnas.1203110110.
[18] C. Zitzmann, L. Kaderali, A.S. Perelson, Mathematical modeling of hepatitis C RNA replication, exosome secretion and virus release, PLoS Comput. Biol. 16 (11) (2020) e1008421, https://doi.org/10.1371/journal.pcbi.1008421.
[19] A.U. Neumann, N.P. Lam, H. Dahari, et al., Hepatitis C viral dynamics in vivo and the antiviral efficacy of interferon-alpha therapy, Science 282 (5386) (1998) 103–107, https://doi.org/10.1126/science.282.5386.103.
[20] M.A. Nowak, R.M. May, Virus Dynamics, Oxford University Press, Oxford, 2005.
[21] R. Bartenschlager, V. Lohmann, Replication of hepatitis C virus, J. Gen. Virol. 81 (7) (2000) 1631–1648, https://doi.org/10.1099/0022-1317-81-7-1631.
[22] C.J. Browne, S.S. Pilyugin, Global analysis of age-structured within-host virus model, Discrete and Continuous Dynamical Models 18 (8) (2013) 1999–2017, https://doi.org/10.3934/dcdsb.2013.18.1999.
[23] P. Magal, Compact attractors for time periodic age-structured population models, Electron. J. Differ. Equ. 65 (2001) 1, https://doi.org/10.1023/A:1011257222927.
[24] G. Gripenberg, S.O. Londen, O. Staffans, Volterra Integral and Functional Equations, Cambridge University Press, 2013.
[25] Z. Feng, M. Iannelli, F.A. Milner, A two-strain tuberculosis model with age of infection, SIAM J. Appl. Math. 62 (5) (2002) 1634–1656, https://doi.org/10.1137/S003613990038205X.
[26] L. Rong, Z. Feng, A.S. Perelson, Mathematical analysis of age-structured HIV-1 dynamics with combination antiretroviral therapy, SIAM J. Appl. Math. 67 (3) (2007) 731–756, https://doi.org/10.1137/060663945.
[27] L. Rong, Z. Feng, A.S. Perelson, Emergence of HIV-1 drug resistance during antiretroviral treatment, Bull. Math. Biol. 69 (6) (2007) 2027–2060, https://doi.org/10.1007/s11538-007-9203-3.
[28] L. Rong, R.M. Ribeiro, A.S. Perelson, Modeling quasispecies and drug resistance in hepatitis C patients treated with a protease inhibitor, Bull. Math. Biol. 74 (8) (2012) 1789–1817, https://doi.org/10.1007/s11538-012-9736-y.
[29] L. Rong, J. Guedj, H. Dahari, et al., Analysis of hepatitis C virus decline during treatment with the protease inhibitor danoprevir using a multiscale model, PLoS Comput. Biol. 9 (3) (2013) e1002959, https://doi.org/10.1371/journal.pcbi.1002959.
[30] L. Rong, H. Dahari, R.M. Ribeiro, et al., Rapid emergence of protease inhibitor resistance in hepatitis C virus, Sci. Transl. Med. 2 (30) (2010) 30ra32, https://doi.org/10.1126/scitranslmed.3000544.